CORROSION FATIGUE CRACK GROWTH BEHAVIOR AT NOTCHED HOLE IN 7075-T6 UNDER DIFFERENT BIAXIAL STRESS RATIOS

THESIS

Alghamdi, Khalid Ali

Captain, Royal Saudi Air Force, RSAF

August 2016

DEPARTMENT OF THE AIR FORCE

AIR UNIVERSITY

AIR FORCE INSTITUTE OF TECHNOLOGY

Wright-Patterson Air Force Base, Ohio

DISTRIBUTION STATEMENT A

AFIT-ENY-MS-16-S-051

CORROSION FATIGUE CRACK GROWTH BEHAVIOR AT NOTCHED HOLE IN 7075-T6 UNDER DIFFERENT BIAXIAL STRESS RATIOS

THESIS

Presented to the Faculty

Department of Aeronautics and Astronautics

Graduate School of Engineering and Management

Air Force Institute of Technology

Air University

Air Education and Training Command

In Partial Fulfillment of the Requirements for the

Degree of Master of Science in Materials Science

Alghamdi, Khalid Ali
Captain, Royal Saudi Air Force, RSAF

Aug 2016

Abstract

This thesis presents the results of a study to quantify the effects of biaxial loading on fatigue crack behavior in both air and saltwater (3.5% NaCl) environments from pre-cracked notched circular hole in a 7075-T6 cruciform specimen using a fracture mechanics approach. With stress ratio of R = 0.5, the crack growth behavior was investigated under fatigue loading with biaxial stress ratio λ of 0.5, 0, -0.5, and -1. The crack propagation was monitored using optical microscopy. Finite Element Analysis was performed using the different stress ranges and stress ratios with various crack sizes to compute stress intensity factors range (ΔK) at the crack tips. It was observed from the study that negative biaxiality has a very pronounced effect on the crack growth rate. The crack propagates faster with negative biaxiality and also the saltwater environment accelerates the crack propagation due to corrosion.

Acknowledgments

First, I would like to express my sincere appreciation to my advisor, Dr. Shankar Mall, for his continuous support and guidance throughout my thesis. His vast knowledge and encouragement were essential to the successful completion of this research

Also, I would like to thank and Dr. Heath Misak for sharing his knowledge and showing me how to capture the SEM images of the fatigue specimens and Dr. Victor Perel for showing me how to properly prepare specimens and perform the experiment, and his help in developing the finite element models by using Abaqus program.

I would like to thank my parents for their love and prayers for me, and most importantly, I would like to thank my wife and my daughter for their support, encouragement, and quiet patience.

Alghamdi, Khalid Ali

Table of Contents

List of Figures

Figure Page

List of Tables

List of Symbols

Symbol	Definition
Δ	change in a variable (unit less)
a	crack length (mm)
α	angle between the y-axis and the crack (degree)
φ	angle between the x-axis and the crack ($\varphi = \frac{\pi}{2} - \alpha$) (degree)
b	width of specimen (mm)
C	constant for Paris law (unit less)
CF	corrosion fatigue
da/dN	rate of crack growth per cycle (mm/cycle)
DOD	Department of Defense
G	strain energy release rate
I	mode one (opening)
K	stress intensity factor (MPa*m^0.5)
M	molar mass
R	stress ratio for cyclic loading (unit less)
r	radius of the circular hole (m)
SCC	stress corrosion cracking
$\sigma_{\theta\theta}$	normal stresses near the crack tip at an angle of $\theta + 90°$ from the local rectangular coordinate system ($x'y'$ plane) and with respect to the local polar coordinate system ($\rho\theta$ plane) (N/m^2)
t	thickness of specimen (mm)

w	width of specimen (mm)
ω	frequency of the applied load
σ	stress (MPa)
λ	biaxial stress ratio

CRACK INITIATION AND GROWTH NATURE AT NOTCHED HOLE IN 7075-T6 UNDER DIFFERENT BIAXIAL STRESS RATIOS

I. Introduction

1.1 Corrosion

Corrosion is one of the wide spread concerns, especially when we want to increase the efficiency of the metal products or decrease the operation cost. It is almost an inevitable impasse in most of the infrastructures. Infrastructure and transportation suffer from the metallic corrosion, because of the major role that it plays in the strength, efficiency and cost of system [12].

Approximately, United States loses 3.1% of its Gross National Product to the corrosion each year, which is almost $276 Billion [9, 12]. Yearly, the transportation division alone pays around $29.7 billion for corrosion damages, and this is 21.5% of the total cost that United States pay for corrosion [9]. These losses indicate that the corrosion needs to be handled more. Figure 1.1 shows that corrosion impacts almost every industry sector [2].

The United States Department of Defense has made a strategy to fight corrosion throughout its forces [13]. DODs' resources have been directed toward corrosion prevention. Also, it started to look into acquisition level before manufacturing, management decisions, maintenance procedures, and sustainment to extend the life of materiel [13]. DOD pays $22.5 billion each year to prevent corrosion and searches for new corrosion solutions and prevention technologies, procedures, products, and management systems for its armed forces and infrastructure [13, 14].

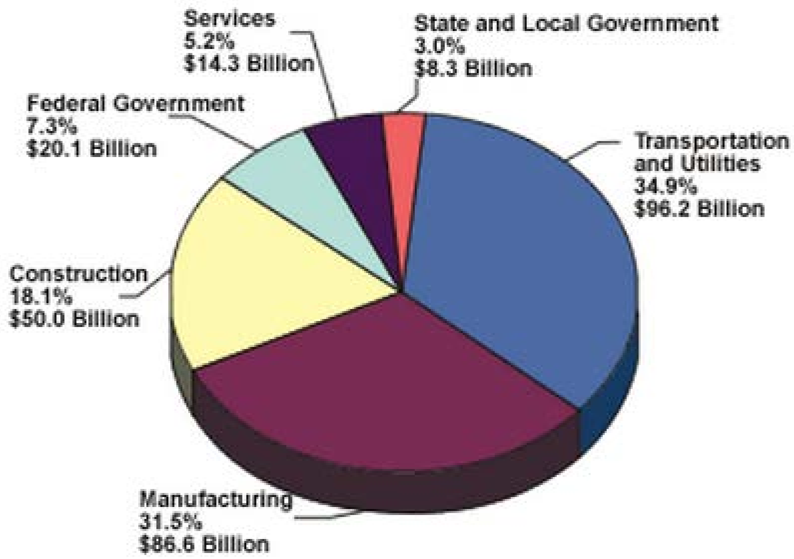

Figure 1.1: Cost of Corrosion in Different Categories of Industry [2].

Corrosion can be defined as deterioration of a metallic material due to the reaction between the metal and its environment [29]. There are many ways to control the corrosion, such as painting, coatings, chemical inhibitors and materials selection. The understanding of the type of corrosion is the way to choose which method is suitable to control it [29, 33].

Aluminum alloy is used in this study and it is most common metals that being used in the aircraft industries, because of its light weight, low cost and its resistance to corrosion. However, aluminum alloy could be effected by corrosion if subjected to acidic solutions. [23]

1.2 Corrosion Fatigue

Fatigue is the failing of a material due to applying of repeating load under the yield point of that material. There are several factors that contribute to fatigue failures, such as applied cyclic stresses, thermal expansions and contractions, poor assembly, welding, and casting [31]. When these different factors failure modes are combined, the failure occurs sooner. Corrosion fatigue (CF) occurs when the crack generated by the repeating load and corrosion at the same time. The material fails faster by the corrosion fatigue than cycles loading only [2]. Corrosion fatigue could lead to catastrophic failure if the cracks are not observed by inspectors in time [10].

1.3 Biaxial Corrosion Fatigue

Aircraft structure fails due to corrosion fatigue, however the way to eliminate the failures is to understand how these failures occurs at the beginning. Then by eliminating, preventing or at least delaying the reasons, the materials performance will be enhanced and that will decrease the cost of operations and increase the lifetime of the aircraft.

During the operation of an aircraft, the aircraft structures experience different types of loads and moments in different directions. If the structures experience these loads and moments in a corrosive environment, the initiation and the propagation of cracks will be accelerated, which could result in corrosion fatigue failure. Accordingly, crack initiation and propagation in a corrosive environment is one of the most important topics that need to be addressed and understood in order to prevent the failures associated with it. A very important approach that has been used a lot to examine the propagation of cracks is the damage tolerance approach. This approach is used to study the crack propagation, and follows the assumption that flaws are present in all structures and propagate due to cyclic loading and corrosion. Through the application of the principles of fracture mechanics, this approach is universally used in aerospace engineering to manage the extension of cracks in structure [24].

Researchers have already started studying crack propagation and the affect of environments on the crack growth behavior [24]. In this time, a lot of data has been documented from those studies, but most of the studies had been done under uniaxial loading [5, 7, 24]. Almost all aircraft structures are subjected to mixed mode of stresses, which can limit the benefits gained from the data of the uniaxial fatigue tests.

The most common loading conditions on aircraft structures is in-plane biaxial loading. A lot of information will be gained from conducting tests in these loading states, which help understanding crack growth rate [24].

Corrosion fatigue crack growth for aluminum alloys and in corrosive (saltwater) environment has been investigated under uniaxial loading conditions, but none of these studies tried to conduct a test under biaxial loading conditions in a corrosive environment [24]. Several studies of an in-plane biaxial fatigue crack growth of aluminum alloy had been conducted in saltwater environment to give a better understanding of crack growth rate generated from rivet holes or bolted joints [25]. In addition, earlier studies have shown that biaxial loading has an influence on fatigue crack growth rates [16, 25].

1.4 Problem Statement

Almost 70% of fatigue cracks start growing from rivet holes or bolted joints Fatigue. That is why the cracks around holes should be examined [20]. In recent years, many experimental studies have been conducted on fatigue crack growth under various biaxial loading conditions [10, 24, 25, 26]. Lately, in-plane biaxial fatigue tests in saltwater environment have been started to be conducted [24, 25]. Many of these studies have focused on positive biaxial loading cases. No conclusive study has been reported out yet that accurately quantifies the influence of negative biaxiality on fatigue crack growth behavior. This is area of focus of this research, using fracture mechanics approach.

A specimen of 7075-T6 aluminum alloy was examined under in-plane biaxial loading in both ambient air and saltwater (3.5% NaCl) environments with 0.5, 0, -0.5, and -1 biaxial stress ratio λ. After that, the results have been compared between positive biaxial loading cases and negative biaxial loading cases having the same experimental setup, to study the effect of negative biaxiality on fatigue crack growth behavior, which is what has been lacking in this field up to now.

Cruciform specimens were made from a 3.18 mm thick sheet of 7075-T6 aluminum alloy to conduct the experiments. Length of the specimen's arm was 120 mm, and width was 45 mm. The radius of curvature at the junction of arms was 28 mm and a hole of 3 mm was drilled at the center. Then, a notch with 1 mm length and 0.25 mm width was machined on the edge of the hole at 0° to horizontal arm. These specimens have stress ratio of 0.5 (R = 0.5). Lastly, a precrack was made from the notch.

The crack growth rate has been measured with the number of cycles to failure. Then, finite element analysis was carried out to calculate the intensity factor range, ΔK. After that, ΔK was linked with the crack growth rate in order to study the behavior of the cracks.

This research provided a great deal of valuable and usable information for fatigue crack growth behavior from a notched hole and will make useful data to compare different biaxial loading conditions in different environments, to better calculate the lifespan of an aging fleet of aircrafts. Also, this study will help to fill the missing part from the previous studies in this field.

II. Background

2.1 Fatigue

There has been a steady increase in the number of military airplanes, commercial airplanes, and unmanned aerial vehicles. With the increased number of aircraft, there is a need to enhance the structural integrity analysis of the old airplanes. The advent of fracture mechanics is a blessing in disguise as it has been applied in the design of aircraft structures. Every aircraft structural component is usually assumed to be having a crack within it. As the aircraft ages, the cracks usually increase in size with time (fatigue) [1].

There is a correlation between fatigue and structural integrity. The disaster in Comet aircraft, for instance, arose due to a crack that grew big enough thus promulgating in an unsteady manner as per the Griffith theory [34]. Fatigue refers to a steady expansion of cracks caused by cycling loads, if the stress falls below the yield point of the material [5, 32]. Fatigue failure can be caused by many types of stress types such as torsion, bending, and rotation [34].

Fatigue in metals begins at surface locations with concentrated stress. It first begins with shear flow along slip planes, and then graduates by generating intrusions and extrusions that the same particular slip, leaving minor steps on the surface. The small steps grow to intensify stress in the particular area and causes the formation of microcracks [30, 31, 34]. The planes of high shear stress experience microcracks more than other regions. The angle is usually 45 degrees to the direction of the load. This is just the first phase, and the second phase occurs when the small voids join and spread through the structure, thus creating a 90 degrees angle crack to the load direction. Finally, the third phase of the fatigue failure occurs when the resistance is exceeded, and a structure occurs, Figure 2.1 [30].

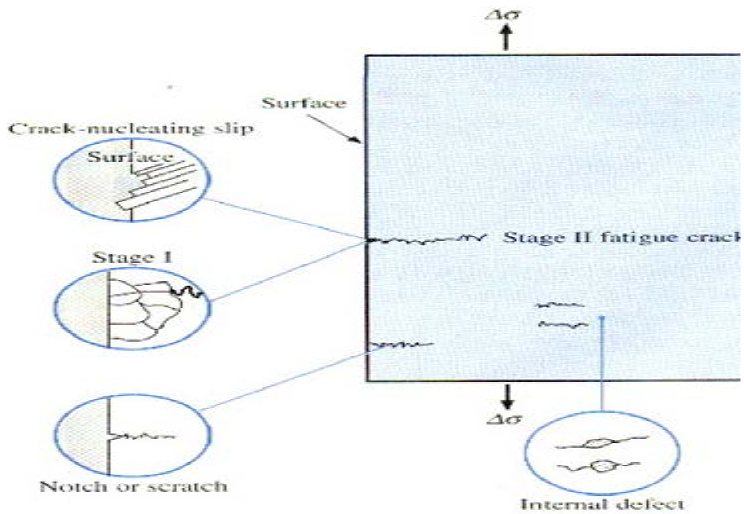

Figure 2.1: Intrusion and Extrusion of Fatigue Crack Initiation [30].

2.2 Corrosion Fatigue

Corrosion fatigue (CF) is one of the most complicated topics of the aircraft structure failure. CF is a variable that needs to be tested for components of aircraft and other structures in the aerodynamic industry because CF is the mechanical breakdown of the materials like the aluminum alloys used in the construction of the structures when they are in a corrosive environment [20, 22]. In other words, the metals used to construct aircraft undergo harsh combinations of stress in the form of loadings and are often in corrosion-causing environment that leads to metals corrosion fatigue [20, 22]. Stress and corrosive environment can cause CF when aircraft components experience them separately or both at the same time. The stress is caused by repeating loading cycles that buildup stress on portions of a metal structure plus the damage caused by a corrosive environment on the same spot [10, 34]. In real life environments a part of a structure becomes weaker when something causes a hole, notch and other similar flaws in the component. Therefore testing the components is necessary to make sure that materials used to construct aircraft and aerospace products must be done to guarantee reliability, durability and safety. Life predictions are made by testing aluminum alloy components for how they act under conditions of uniaxial cyclic, biaxial cyclic, out-of-phase and irregular loads as well as corrosive environments [20, 22].

The definition of corrosion fatigue is the damage that results in a corrosive environment on a metal structure from repetitive loading cycles and buildup of the load caused by the cycles [10, 34]. Components are tested for corrosive environments by placing them in a chamber with saltwater containing 3.5% NaCl (sodium chloride) [26, 27]. The damage becomes worse over time and four stages can be identified during the process:

1. Cycle plastic deformation.
2. The initiation of microcracks.
3. Small crack growth from the microcracks.
4. The enlargement of small crack growths into larger cracks and finally into macrocracks [10].

Mechanical engineers study corrosion fatigue mechanisms and fractography of aluminum alloy metals in laboratories because modes of failure that cause damage must be prevented. Research is done to prevent corrosion fatigue by learning details of the processes involved. Two of the mechanisms, hydrogen embrittlement and film rupture, are the main causes researchers identify as causing corrosive fatigue, therefore those mechanisms are studied very closely [5]. This research study is focused on the mechanism of hydrogen embrittlement of the aluminum metal alloy 7075-T6. In other words this study looks at the hydrogen embrittlement process from start to finish on the aluminum metal alloy 7075-T6 while it is causing corrosion fatigue failure [11].

A flaw in the metal that causes a hole through the protective coating material of a metal surface and reaches the surface allows the initiation of hydrogen entitlement such as a notch. Avoiding all flaws is the ideal situation, because when the surface is exposed to the environment, even a very small amount, corrosion is expected to occur. An open space in protective coating that allows the environment to reach the surface allows the production of hydrogen ions. The hydrogen ions are the source that causes weakening of metallic binding within the metal structure.

After reaching the surface of the alloy through the flaws, the hydrogen ions start entering the alloy’s lattice metal structure until embrittlement results. When embrittlement occurs, the metal alloy becomes brittle and as the process of embrittlement continues, the more brittle the metal alloy structure becomes [5]. Figure 2.2 provides an overview of the mechanism of corrosion fatigue [5].

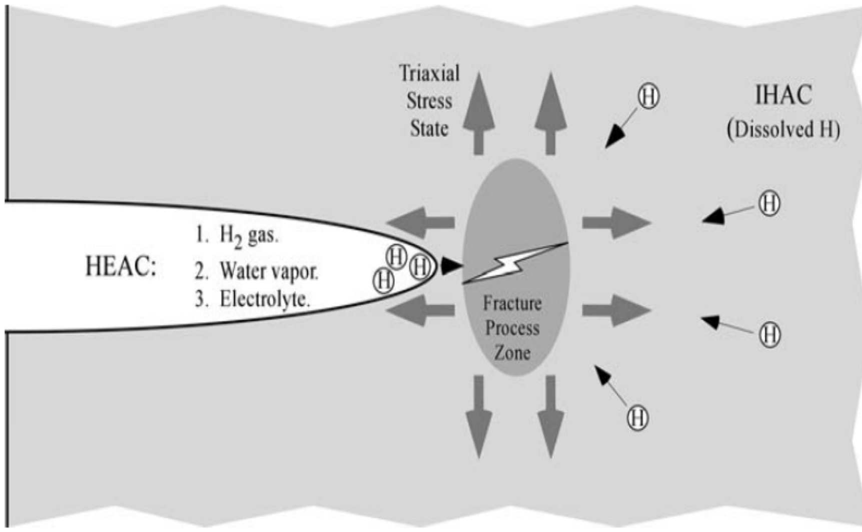

Figure 2.2: Mechanism of Corrosion Due to Hydrogen Embrittlement [5].

Transgranular cracks are initiated by the hydrogen embrittlement [5, 31]. Repeated loading cycles enhance the propagation of the cracks in the grain of the alloy [5, 31]. If a notch has a sharp V-shape at its root and other conditions are favorable transgranular cracks occur. Corners in a flaw are also the originating site of a transgranular crack under coating, therefore coatings are not foolproof. Even under coatings the cracks can form and grow [31]. Interpreting the laboratory stress test by inputting measurement results and inputting them into computer models to simulate the mechanisms helps gain more information from the corrosion fatigue mechanism from hydrogen embrittlement [10, 11]. Computer model simulations of the mechanisms are described in more detail in Chapter 3. Ductile, cleavage and intergranular fractures are all examples of micromechanisms seen in metal corrosion fatigue [5]. The mechanisms are described below, because an understanding of how corrosion fatigue happens is needed for making sense of laboratory results [10, 11].

CF and stress corrosion cracking (SCC) are similar mechanisms for crack formation and fractures when embrittlement is present. Nevertheless, they are also different based on loading types and amounts. SCC results from static loading. CF results from fluctuating loading. SCC and CF also look different, the appearance of surface cracks looks like cleavage in SCC and striations (or benchmarks) in CF. The shape of the cracks (also known as the morphology) is also different between SCC and CF. SCC shows branched cracks while CF is characterized by a blunt tip appearance [43].

2.3 Corrosion Effect on Fatigue Life

A cyclic loading and a corrosive environment together cause more damage when compared to corrosion and cyclic loading that occur separately. The combination of the corrosive environment and the cyclic loading on metal structures causes synergistic damage [42]. Notches are mad from intrusion and extrusion processes produced from the fatigue loading [42]. Add to that situation a corrosive environment, then oxidation occurs at the metal surface of the notches [42]. And then, the corrosion does become inactive for a time as more damage is caused to by fatigue. The fatigue causes a negative impact on the passive layer of the material so that the corrosion has a new exposed surface to attack. The process causes a highly reduced fatigue life [42].

Fatigue life and fatigue limit need to be understood because they are commonly used to interpret laboratory results caused by fatigue. Corrosion cracking caused by stress and other crack growth factors relate to time factors and must be taken into account when predictions are made [5]. Fatigue life is measured by how many cycles lead to the failure of a component [18]. Fatigue limit refers to the maximum value of all the alternating stresses that are survived with no failure by a component [18]. In a corrosive environment both fatigue life and fatigue limit are reduced [18]. The negative effects of corrosion on a structural component's fatigue life are expressed as Damage ratio [18].

$$\text{Damage Ratio} = \frac{\sigma_{cf}}{\sigma_f} \tag{2.1}$$

where

σ_{cf} = Corrosion fatigue strength, and

σ_f = Fatigue strength in a neutral environment [18].

Corrosion fatigue is represented by low values for maximum stress and failure in a short period of time for the metal or alloy structural component. The amount of stress and the numbers of stress cycles in a corrosive environments lead to the fatigue limit. See Figure 2.3.

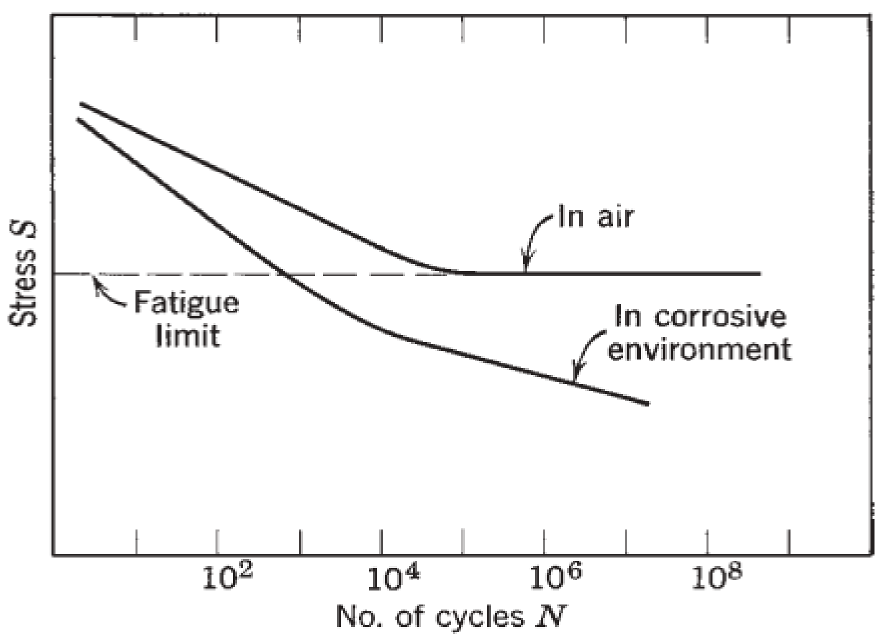

Figure 2.3: The Effect of Environment on the Fatigue Limit of a Material [42].

Several ways to prevent corrosion fatigue are available such as design of the aluminum alloy, design of the structure, the construction process of the component, the amount of loading and knowing the environment expected [18]. Therefore tests that can help predict how the component will react to CF are practical as well as necessary. The design and construction of the metal and metal alloy components, when properly carried out can reduce the damage. Techniques like shot peening (SP), laser peening (LP), and low plasticity burnishing (LPB) enhance the performance under compressive residual stresses according to some researchers [35]. The flaws like notches and rough surfaces need to be avoided as much as possible in order to prevent corrosion fatigue to a large degree [18]. Treating the component according to its ability to perform is helpful, so applying only the minimum cyclic loading, keeping the environment clean of corrosion-inducing factors and using protective coatings that prevent corrosion are all used in the industry [18].

2.4 Fracture Mechanics

Mechanical performance of structure components can be enhanced by studies in fracture mechanics that research the details of crack propagation [34]. The fracture mechanics requires stress and strain analysis of elastic and plastic components that have known flaws and cracks. The purpose is to predict the macroscopic failure in components [5]. The core of fracture mechanic is to predict the crack growth behavior. Crack can experience there type of loading, see Figure 2.4 [5]:

- Opening mode, Mode I: the principle load is applied normal to the crack plane, tends to open the crack,

- Sliding mode, Mode II: corresponds to in-plane shear loading and tends to slide the one crack face with respect to the other, and
- Tearing mode, Mode III: refers to out-of-plane shear [5].

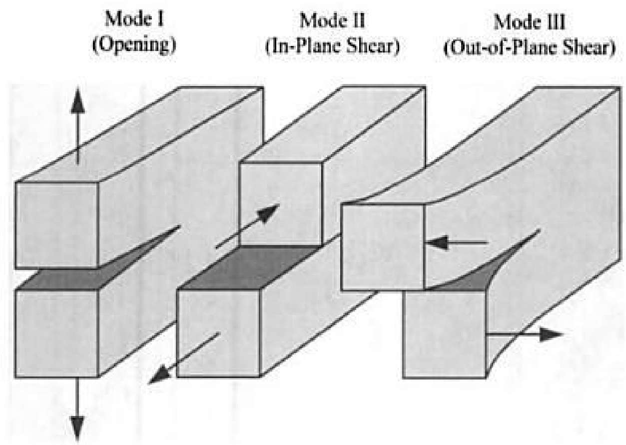

Figure 2.4: The Three Modes of Loading That Can Be Applied to a Crack [5].

Depending upon the circumstances a crack may be exposed to only one mode or exposed to two or to three of the mode types listed above [5]. For mode I and mode II the stress field that is just in front of the crack tip are isotropic and linear elastic material [5].

In the current study, the mode studied is Mode I loadings. The reason Mode I was chosen due to the characteristics of the experiment being studied. The experiments for the current research were designed to cause Mode I loading. A more detailed description is found in Chapter 3, the methodology chapter.

In this study, the cracks in AA7075-T6 were propagated from a circular hole in the thin cruciform experimental material under biaxial loading. The material was prepared for the experiment by notching and afterwards pre-cracking the material. The purpose of the research is to study the crack propagation from the circular hole and to determine the propagation direction. The next sections are dedicated to a literature review on characteristics such as cracks starting from a circular hole and the stress intensity factor, stress transformation, global coordinate system, local coordinate system and the crack propagation direction. An analytical study for the prediction of the crack propagation direction is also discussed below.

2.4.1 Stress Intensity Factors for a Crack Initiated From a Circular Hole in Thin Plate under Biaxial Loading

The stress intensity factor is identified near the crack tip and the stress state at that location [5]. If a crack is initiated from a circular hole in a thin plate (plane stress condition) then, the stress intensity factors for mode I and II are given by the following expressions [17]:

$$K_I = \frac{\sqrt{\pi r}}{2\sqrt{2}} \sqrt{\frac{l_0\,(l_0 + 2)^3}{(l_0 + 1)^3}}\ (S_{yy} + S_{xx} - (S_{yy} - S_{xx}) \cos 2\alpha) \qquad (2.2)$$

and

$$K_{II} = \frac{\sqrt{\pi r}}{2\sqrt{2}} \sqrt{\frac{l_0\,(l_0 + 2)^3}{(l_0 + 1)^3}}\ (S_{xx} - S_{yy}) \sin 2\alpha) \qquad (2.3)$$

where

$$l_0 = \frac{1}{2}\left(-1 + \frac{a}{r} + \sqrt{2\frac{a}{r} + \frac{a^2}{r^2} + 1}\right) \qquad (2.4)$$

where:

S_{xx} is the nominal stress at a large distance from the crack tip in the x-direction (N/m^2).

S_{yy} is the nominal stress at a large distance from the crack tip in the y-direction (N/m^2).

r is the radius of the circular hole (m).

a is the length of the crack (m).

α is the angle between the y-axis and the crack.

φ is the angle between the x-axis and the crack ($\varphi = \frac{\pi}{2} - \alpha$).

Figure 2.5 shows a crack initiated from a circular hole, subjected to biaxial remote stresses ($S_x$and S_y) with respect to the global rectangular (x and y) coordinate system.

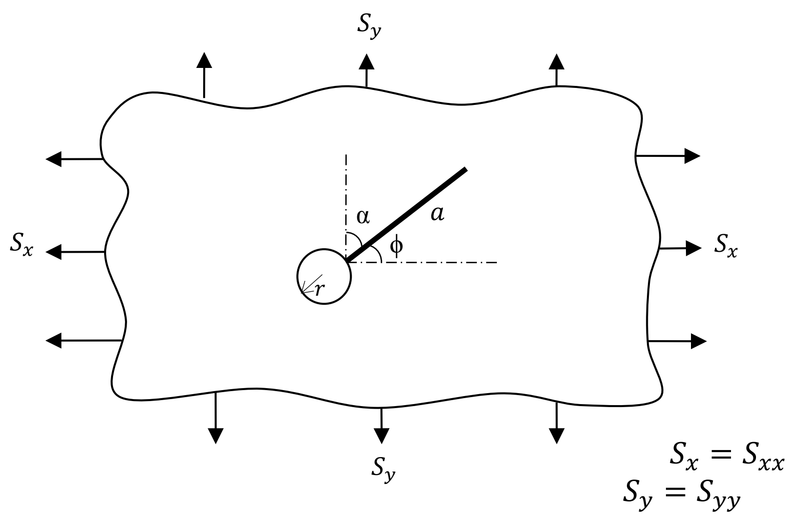

Figure 2.5: A Crack Initiated From a Circular Hole While Subjected to Biaxial Remote Stresses.

Now, when the angle α between the y-axis and the crack is 90° as in the case of this study, then equations (2.2) and (2.3) become [17]:

$$K_I = \frac{\sqrt{\pi r}}{2\sqrt{2}} \sqrt{\frac{l_0\,(l_0\ + 2)^3}{(l_0\ + 1)^3}}\ (S_{yy} + S_{xx}) + (S_{yy} - S_{xx}) \tag{2.5}$$

and

$$\mathrm{K_{II}} = 0 \tag{2.6}$$

2.4.2 Direction of Crack Propagation

Erdogan and Sih consider the stress component $\sigma_{\theta\theta}(\theta)$ as the maximum value, when $\theta = \theta^*$, which is $\sigma_{\theta\theta}(\theta)$ takes the maximum value causing the crack propagation towards the direction of angle $\theta = \theta^*$ [8]. Other researchers tried to predict the direction of the crack propagation with the results shown below:

Sih Cha [37, 38]:

$$\theta^* = -2\frac{\mathrm{K_{II}}}{\mathrm{K_I}} - \frac{2\varkappa - 30}{9 - 3\varkappa}\left(\frac{\mathrm{K_{II}}}{\mathrm{K_I}}\right)^3 + \cdots \tag{2.7}$$

where

$$\varkappa = \begin{cases} 3 - 4\nu & \text{for plane strain} \\ \dfrac{3 - \nu}{1 + \nu} & \text{for plane stress} \end{cases} \tag{2.8}$$

and ν is the Poisson's ratio.

Berezhnitski and Gromyak criterion [6]:

$$\theta^* = -2\frac{\mathrm{K_{II}}}{\mathrm{K_I}} - \frac{168 - 2(\varkappa - 1)^2}{36 - 3(\varkappa - 1)^2}\left(\frac{\mathrm{K_{II}}}{\mathrm{K_I}}\right)^3 + \cdots \tag{2.9}$$

Tian, Lu and Zhu criterion [40]:

$$\theta^* = -2\frac{\mathrm{K_{II}}}{\mathrm{K_I}} + \frac{20\varkappa - 6}{3\varkappa}\left(\frac{\mathrm{K_{II}}}{\mathrm{K_I}}\right)^3 + \cdots \tag{2.10}$$

Tiroshu criterion [41]:

$$\theta^* = -2\frac{K_{II}}{K_I} + \frac{20}{3}\left(\frac{K_{II}}{K_I}\right)^3 + \cdots \tag{2.11}$$

In this study, thin specimens (plane stress condition) of aluminum alloy 7075-T6 used for which the young’s modulus E and the Poisson’s ratio ν are [1]:

$$E = 7.17 \times 10^{10}\mathrm{Pa}, \qquad \nu = 0.33 \tag{2.12}$$

which make

$$\varkappa = \frac{3-\nu}{1+\nu} = 2.0075 \tag{2.13}$$

the previous formulas becomes:

Erdogan and Sih criterion:

$$\theta^* = -2\frac{K_{II}}{K_I} + 4.6667\left(\frac{K_{II}}{K_I}\right)^3 + \cdots \tag{2.14}$$

Sih Cha criterion:

$$\theta^* = -2\frac{K_{II}}{K_I} + 8.7271\left(\frac{K_{II}}{K_I}\right)^3 + \cdots \tag{2.15}$$

Berezhnitski and Gromyak criterion:

$$\theta^* = -2\frac{K_{II}}{K_I} + 5.0363\left(\frac{K_{II}}{K_I}\right)^3 + \cdots \tag{2.16}$$

Tian, Lu and Zhu criterion:

$$\theta^* = -2\frac{K_{II}}{K_I} + 5.6704\left(\frac{K_{II}}{K_I}\right)^3 + \cdots \tag{2.17}$$

Tiroshu criterion:

$$\theta^* = -2\frac{K_{II}}{K_I} + 6.6667\left(\frac{K_{II}}{K_I}\right)^3 + \cdots \tag{2.18}$$

Because K_{II} is equal to zero equation (2.6) and the crack lies on a principle plane and subjected to Mode I loading, the crack propagation angle is zero.

2.5 Fractography

In general, fractography is the study of material surfaces that have been fractured due to stress, loading, environment, or other reasons [28]. Fractography is a high technology science that uses a variety of instruments like high powered microscopes and scanning electron microscopes to carry out failure analysis. Fractography is used during testing in order to learn the types of causes of failure so they can be avoided in finished components. The major use of fractography is to better understand and predict crack growth behavior.

2.6 Previous Research

The combination of corrosion and fatigue can cause fatal accidents and that is why research on failure behavior due to those two factors is so important. Material science laboratories contain experimental equipment to test materials and better understand failure behavior. Laboratory studies control certain factors to learn the effects of a variety of materials and loadings. For example, fatigue testing instrument was used as early as 1985 to study crack growth behavior for the two aluminum alloys, 7075-T6 and 2024-T3 [22].

In the 1960s the first study for the stress intensity factor range (ΔK) versus the crack propagation rate (da/dN) was carried out [19]. The number and types of research are growing due to the importance of safety in the aerospace program as well as other industrial projects. As technology and computer capacity increases more complex research is possible. For example crack propagation and the influence of environment on the growth and behavior of cracks is commonly investigated for materials [24]. Research results are published and relied upon, but not all areas for study have been well-documented. The area that has been most studied is on the topic of uniaxial fatigue conditions, so more research is needed on mixed mode of stresses, which is necessary for most aircraft structures [5, 7, 24]. Recently studies rely upon biaxial fatigue test instrumentation for research on crack growth behavior assuming ambient air and saltwater (3.5%) conditions in-plane. The research is carried out from the perspective of fracture mechanics using cruciform-type specimens. The next paragraphs discuss some of these studies.

2.6.1 Biaxial Stress Ratios

7075-T7351 and 2024-T351 aluminum alloys were materials that were studied to learn about fatigue crack growth behavior when center-cracked cruciform specimens were the samples [21]. The conditions applied were biaxial loading under a variety of biaxial stress ratios ($-1.5 \leq \lambda \leq 1.75$ for constant amplitude tests, $-0.5 \leq \lambda \leq 0.5$ for periodic single overload and spectrum load test) [21]. The three main results of the study are listed below.

- A relationship between the crack direction and the impact of the stress component was identified; a parallel stress component applied in equal or smaller amounts than a specimen receives under normal conditions at the crack direction causes the crack to grow in a straight line [21].

- The biaxiality ratio has an influence when the specimen experiences a stress parallel to the crack; under such conditions the crack growth rates were shown to range from small to negligible dependent of the value of the biaxiality ratio [21].
- A large biaxial stress component behaves as the controlling factor for the crack growth rate [21].

Therefore it was learned that the crack growth rate depended directly upon larger biaxial stress values.

2.6.2 Notched and un-notched specimens

A servo-hydraulic testing machine was used to study fatigue cracks propagation to observe the biaxial stresses for two types of materials, un-notched and central circular notched plates [15]. The servo-hydraulic testing machine did not allow vertical and horizontal cycles to take place simultaneously [15]. Therefore the research was carried out by holding the horizontal stress stationery and cycling the vertical stress at three variations: when λ are equal to -1, 0 and 1. Two other conditions were used in each experiment; measurements of crack length were taken with a microscope and curve-fitting technique [15]. The experiment results showed that when decreasing tensile loading occurs parallel to the crack, then the crack growth rates; meanwhile, compressive loading resulted in crack growth rates.

2.6.3 Biaxial stress & crack growth

Researchers designed changeover tests on steel cruciform specimens with a central crack in order to observe how biaxial stress influences crack growth [4]. The biaxiality ratio was changed after the duration of the experiment reached 50% and λ (the biaxial ratio) used in the current research [4]. The change in the rate of crack rate was recorded [4].

- During biaxial loading applying tensile stress parallel to the crack caused a higher uniaxial loading compared to the crack growth rate [4], but
- During biaxial loading by applying compressive stress parallel to the crack in the specimen; the results showed that the crack rate was higher than during uniaxial loading [4].

2.6.4 Cabin pressure conditions

An experiment for the complex circumstances of a mixed mode internal cabin pressure with gust loading under laboratory conditions [39]. The purpose of the experiment was to observe fatigue crack growth when biaxial quasi-static loads under conditions of constant amplitude [39]. The conditions were applied to the specimens, which were the cruciform test coupons to simulate the “pressurized transport aircraft fuselage panels” that have to work and work safely during flights [39].

The two sets of specimens used for the experiment were formed at different thicknesses. The first set was steel of a 1-mm thickness and the conditions of the experiment held the amplitude at a constant loading. The purpose of a constant amplitude loading was carried out to observe if the process of the testing system was useful [39]. The second set of specimens consisted of 2024-T3 aluminum alloy with a 2.7-mm thickness [39].

Testing for the load spectrum under biaxial loading conditions for CF studies is usually done use the “TWIST load spectrum”. The transport aircraft wing loading for CF is commonly test with Marker-TWIST or variables of the TWIST load spectrum [39]. The aluminum alloy was tested using a modified Marker-MiniTWIST system at different loads [39]. The axial load offsets and the static transverse loadings were different for each sub-set of the experiment. For test numbers 1 through 3 the spectrum used was the Marker-MiniTwist. Test 1 was carried out with an axial load offset of 1.5 kN and a static transverse load of 3 kN. Test 2 was carried out with an axial load offset of 1.0 kN and a static transverse load of 2 kN. Test 1 was carried out with an axial load offset of 0.5 kN and a static transverse load of 1 kN. Test number four was more complicated because three spectrums were used: Marker-MicroTWIST up to 33 mm, Marker-MiniTWIST up to 37 mm, and Marker-Twist up to 40 mm [39]. The axial load offset for test 4 amounted to 1.5kN. The static transverse load was more complex because the researcher "toggled between 0 and 3 kN after each 1 mm crack increment" [39]. The findings were that the amount of biaxiality loading and fatigue crack rates are directly related [39].

2.6.5 Fatigue crack growth & biaxial cyclic loadings

Biaxial cyclic loadings were applied to AK4-1T1 and Al-alloy D16T specimens of on 1.2 to 10 mm thickness to carry out fatigue crack growth experiments [36]. The purpose of the experiment was to test cruciform specimens for fatigue crack growth [36]. The thickness of the research specimens ranged from 1.2 to 10 mm and produced from aluminum based alloys [36]. Loadings during the experiment were carried out under both "constant (regular) and variable (irregular) amplitudes of uniaxial and biaxial loads" with some loadings specifically designed to simulate overloads [36]. Crack closure effects were observed during "rotation instability," blunting effect, crack retardation, and other measurements of effects resulting from the loads [36].

The results of the experiment determined a biaxiality ratio of between -1.4 and +1.5; while the stress ratios ranged from 0.05 to 0.8 [36]. The amplitude cycle was kept constant for some runs and was varied for other cyclic loads [36]. Three conditions were measured plane-stress condition, plane-strain condition and out-of phase loading to simulate the crack closure effects on crack growth [36].

- The results for the plastic zone increased when the phase difference was increased from 0° to 180°; but
- above 108° the plastic zone decreased as the phase difference was raised; and
- The researcher demonstrated that the fatigue cracks increase at a faster rate when the biaxiality stress ratios are large. [36]

2.6.6 Biaxial stress on fatigue variables

The fatigue behaviors of fatigue life, fatigue crack growth, and fatigue crack path were measured in aluminum alloys under conditions of biaxial loadings [20]. Aluminum alloys 1100-H14 and 7075-T651 cruciform specimens with 2 mm in thickness [20]. The plane was a horizontal or a 45° angle from the notch in the center of the specimens [20]. The biaxiality ratio, λ ranged from 0 to 1.5, the stress ratio, R equaled 0.1 and the loading frequency 15 Hz in an ambient air environment [20]. The biaxial load was applied out-of-phase to all the specimens [20]. The results showed that:

- during reduced longitudinal stress then the fatigue life increased when the loading was both in-phase and out-of-phase, on the other hand

- an improved fatigue life resulted for in-phase loading than with the out-of-phase loading (at specific biaxiality ratios) [20].
- The three aspects that were found to influence the path of a fatigue crack during the experiment were the biaxiality ratio, the phase angle and the initial center notch location [20].
- Interestingly the fatigue growth rates decreased when the biaxiality ratio was high and lower the in-phase loading causing fatigue life increases and a small change in biaxiality ratio under out-of-phase conditions [20].

The fatigue crack growth was investigated under the influence of biaxial stresses and a biaxial fatigue testing machine [44]. Center cracks were evaluated in samples of SUS 304 stainless steel for stress intensity factors while applying constant and variable biaxiality stress conditions [44]. The biaxial ratios of λ= -1, 0, and +1 were used, and the stress ratio, R equal to 0.1 [44]. The crack length measurements were made with a travelling microscope [44]. At low stress the biaxiality showed only negligible influence on the crack growth rates, but the effects were noticeable at high stresses [44].

2.6.7 Two environmental conditions compared

The two environments of ambient air and saltwater (3.5% or 0.6 M NaCl) were used in fatigue crack growth experiments with biaxial cycle loadings (that cause stresses) for biaxiality ratios of 1 and 1.5 and the stress ratio set at 0.5 [26, 27]. Aluminum alloy 7075-T6 cruciform specimens, 3.18 mm thick with a 6 mm diameter center hole along with a machined notch measuring 1mm x 0.25mm [26]. The angle of the horizontal to vertical arms was 45° [26, 27]. Pre-cracking of the notch was carried out under conditions of biaxial fatigue loading while the notch and the crack were both perpendicular to the specimens' rolling direction [26, 27]. The crack lengths were measured using an optical microscope system [26, 27]. The stress intensity factors were calculated using a finite element analysis computer model [26, 27].

- When the biaxiality ratio (λ) was equal to 1, the experiment demonstrated crack initiation with a growth path coplanar with the notch system, but if λ equaled less than 1.5 the crack growth path was non-coplanar [26].
- Crack initiation during biaxial fatigue occurred showing a lower crack driving force level compared to increasing the biaxiality ratio, which exhibited a decreased crack initiation driving force [26].
- Under ambient laboratory air conditions the biaxial fatigue (at $\lambda = 1$) and uniaxial fatigue (at $\lambda = 0$) demonstrated the same growth rate [26]. Whereas, at $\lambda = 1.5$ and a specified crack driving force the crack growth rate was higher [26].
- The slowest crack growth rate occurred for uniaxial fatigue in a saltwater environment, but the fastest crack growth rate occurred for biaxial fatigue at λ equal to 1.5 in the same environment; meanwhile
- For biaxial fatigue in saltwater conditions with λ equal to 1 the crack rate growth was between the slowest and the fastest [25].
- Experiments taking place under laboratory ambient air conditions to observe fatigue damage mechanisms showed planar slip when the biaxial ratio equaled zero, wavy slip when the biaxial ratio equaled 1.5, and a combination of wavy and planar when the biaxial ration equaled 1 [25].

- Experiments under a saltwater environment displayed fatigue crack propagation that was transgranular at a biaxial ratio of 1 for both uniaxial and biaxial fatigue [25].

2.7 Purpose of Thesis

The effect on fatigue crack growth experiencing under uniaxial loading conditions. On the other hand, biaxial loading conditions are included in only a few studies in the published literature. The studies reviewed and demonstrated that crack growth rate is influenced by biaxial fatigue.

This research is unique because the aluminum 7075-T6 studied the fatigue crack growth with a negative biaxiality. The aluminum 7075-T6 alloy was observed under the two conditions of ambient air and saltwater (3.5% NaCl) during plane biaxial loading. A comparison was then made to positive biaxiality for studying the effect of changing biaxiality to crack growth rate. This study attempted to fill in the research gap by its design. The study also addressed the fracture mechanics issues to explain the results and also to predict results. The research databases and documents show the experimental results so that corrosion fatigue can be better understood and so corrosion fatigue failure can be addressed.

2.8 Summary

The characteristics of failure due to stress and corrosion have been published for a variety of materials and loading conditions. McEvily (1985) researched crack growth in aluminum alloys 7075-V T6 and 2024-T3 by using a fatigue testing machine [22]. Paris (2007) undertook the stress intensity factor range (ΔK) versus the crack propagation rate range (ΔP) using the ratio da/dN [19]. Recent advances in technology have led to the ability to carry out new studies on failure. Research into the influence of the environment and propagation of cracks on crack growth behavior was one of the first topics [24]. Uniaxial fatigue conditions are those used for most of the experiments but not for those concerning aircraft whereas for aircraft structures [5, 7, 24]. Aircraft components are exposed to stresses in mixed modes, and in that way the benefits from the uniaxial fatigue tests data are limited.

The experimental researches on airplane components are necessary in order to measure and analyze crack growth behavior when the conditions causing fatigue are plane axial loadings. The experiments for this research were done using biaxial fatigue instrumentation. The conditions of the tests for the aluminum alloy components were

- The plane biaxial loading condition,
- Saltwater environment (3.5% or 0.6 M NaCl) and
- Ambient air environment

while using a fracture mechanics approach and cruciform-type specimens.

The methodology chapter below explains the details of the experimental process.

III. Methodology

3.1 Overview

Many examples of uniaxial tests were found in the literature, showing that more biaxial tests are needed. Metal cruciform specimens are better for carrying out biaxial tests in contemporary times so that the prediction of load and the strain are more reliable for real life aircraft components. A cruciform specimen is one with a two dimensional shape because is formed from two uniaxial components at a 90° angles from each other forming a cross [36]. Loadings and a corrosive environment are the causes of CF investigated here. The two causes are responsible for CF when aircraft components are exposed to them separately or at the same time. Therefore the methodology takes a look at the three circumstances of loading, corrosive environment (saltwater 3.5%), or both loading stress and a corrosive environment at the same time.

3.2 Material

The specimens used for this research were made of aluminum alloy 7075-T76. Aluminum is a lightweight material that is very attractive for airplanes because it is so strong and it can be strengthened by additional treatment. Other attractive characteristics are high-quality corrosion and stress resistance and high strength-to-density ratio coupled with other fundamental properties necessary for applications in aircraft construction. Although, the strength-to weight ratio is high in aluminum [3]. Aluminum is a material that can be fabricated into a diverse range of shapes.

The aluminum alloy 7075 is the fundamental material that is the basis for the development of the 7075-T6 alloy [3]. It was developed by the manufacturer Alcoa in

1943, since that time the aluminum alloy series 7XXX was developed throughout the years in materials that the aerospace industry uses for many components [3]. The material so popular with the aerospace industry because of high strength and durable characteristics like moderate toughness that are necessary under the harsh conditions airplanes and other aerospace products need to withstand [3]. The basic composition of aluminum alloy 7075 is aluminum, zinc, magnesium and copper plus chromium [3]. Table 3.1 shows the chemical composition of AA 7075-T6 [3].

Table 3.1: Chemical compositions of AA7075-T6 alloy [3].

Element	**Weight Percentage**
Aluminum	87.1 - 91.4
Zinc	5.1-6.1
Magnesium	2.1-2.9
Copper	1.2-2
Iron	Max 0.5
Silicon	Max 0.4
Manganese	Max 0.3
Chromium	0.18-0.28
Titanium	Max 0.2
Other	each Max 0.05
Other	total Max 0.15

The suffix T6 shows that the aluminum alloy has been tempered by thermal treatment (also known as heat treatments) after that an aging process was used to prepare the finished alloy. Thermal treatments are applied to increase alloy to their optimum toughness and strength along with other practical features [3]. T6 is the temper of the aluminum alloy used in this research because it is typically used for aircraft component construction [3]. The structures for the aerospace industry require components built from aluminum alloy 7075-T6 because of the high strength, low density, moderate toughness and corrosion resistance [3]. Table 3.2 shows AA 7075-T6 mechanical properties [3].

Table 3.2: Mechanical properties of AA 7075-T6 [3].

Mechanical Properties			
	Metric	English	Comments
Hardness, Brinell	150	150	AA; Typical; 500 g load; 10 mm ball
Hardness, Knoop	191	191	Converted from Brinell Hardness Value
Ultimate Tensile Strength	572 MPa	83000 psi	AA; Typical
Tensile Yield Strength	503 MPa	73000 psi	AA; Typical
Elongation at Break	11 %	11 %	AA; Typical; 1/16 in. (1.6 mm) Thickness
Modulus of Elasticity	71.7 GPa	10400 ksi	AA; Typical; Average of tension and compression. Compression modulus is about 2% greater than tensile modulus.
Poisson's Ratio	0.33	0.33	
Fatigue Strength	159 MPa	23000 psi	AA; 500,000,000 cycles completely reversed stress;
Fracture Toughness	20 MPa-m½	18.2 ksi-in½	K(IC) in S-L Direction
Fracture Toughness	25 MPa-m½	22.8 ksi-in½	K(IC) in T-L Direction
Fracture Toughness	29 MPa-m½	26.4 ksi-in½	K(IC) in L-T Direction
Machinability	70 %	70 %	0-100 Scale of Aluminum Alloys
Shear Modulus	26.9 GPa	3900 ksi	
Shear Strength	331 MPa	48000 psi	AA; Typical
Density	2.81 g/cc	0.102 lb/in³	AA; Typical

3.3 Test Specimens Description

The material for the tests consisted of 7075-T6 aluminum alloy sheets measuring 3.18 mm thick from which cruciform specimens were produced. The specimens arm measured 120 mm in length, and an arm width of 45 mm. The radius of curvature of the arm junction measured 28 mm. A hole was drilled into the center of the specimens that were also notched by an electro-discharge method. The notch produced for each specimen was collinear with the horizontal arm and measured 1 mm in length by 0.25 mm width as shown in Figure 3.1. The purpose of the notch was to draw stress concentration. In that way, the crack formed during the experiment at the location of the stress concentration. Also at the machined notch, a pre-crack measuring 1 mm in length was produced lying collinearly to the notch. Stress fatigue was used to for purposes of the pre-cracking so there would be an initial sharp crack. A sharp crack was needed for the initial crack to make sure that the stress intensity factor was meaningful [5].

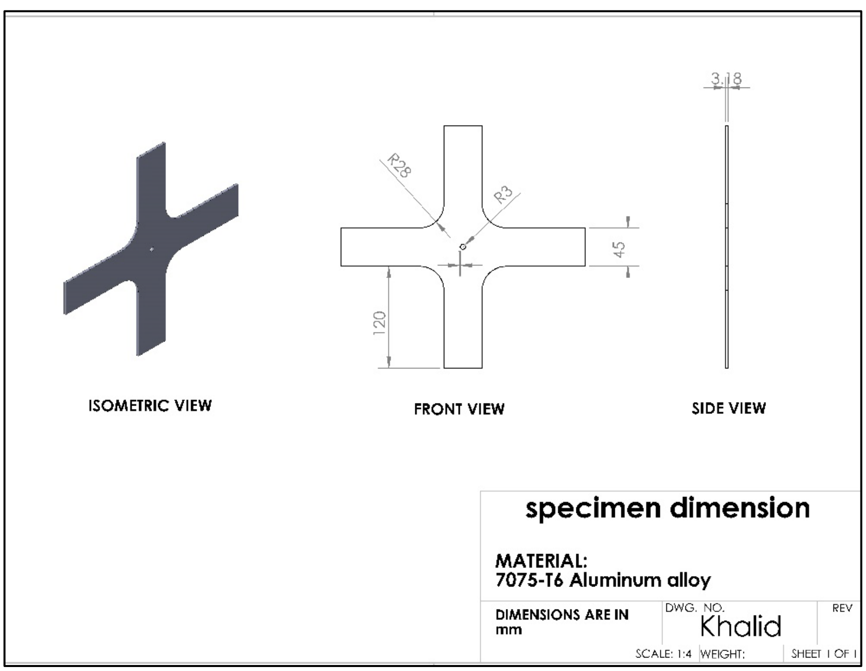

Figure 3.1: Drawing Shows the Specimen Dimensions.

3.4 Test Procedures

The first step of the experiment was to prepare the cruciform specimens. The biaxial experiments were carried out on the laboratory's Material Testing System (MTS). The cyclic biaxial loading was controlled so that the vertical and horizontal loadings were set by the researcher as desired. In that way the biaxial stress ratio was controlled. The stress ratios were equal for both the horizontal and vertical loadings (R_x=R_y=0.5). The loads were applied at the frequency of 10 Hz.

The first sets of experiments were carried out under the condition of ambient laboratory air. Figure 3.2 shows the biaxial experimental setup with a cruciform specimen in air. A second set of experiments were carried out under conditions produced with a chamber containing saltwater (3.5% NaCl), Figure 3.3.

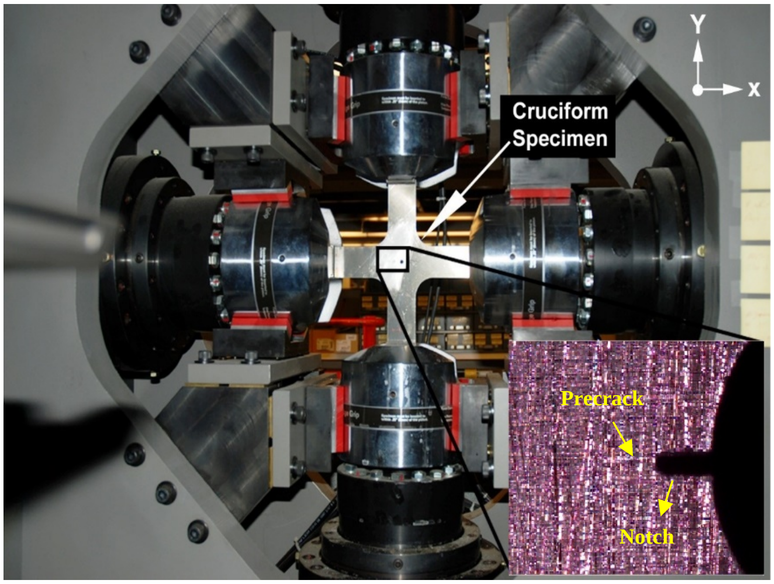

Figure 3.2: The Biaxial Experimental Setup with a Cruciform Specimen in Air Environment.

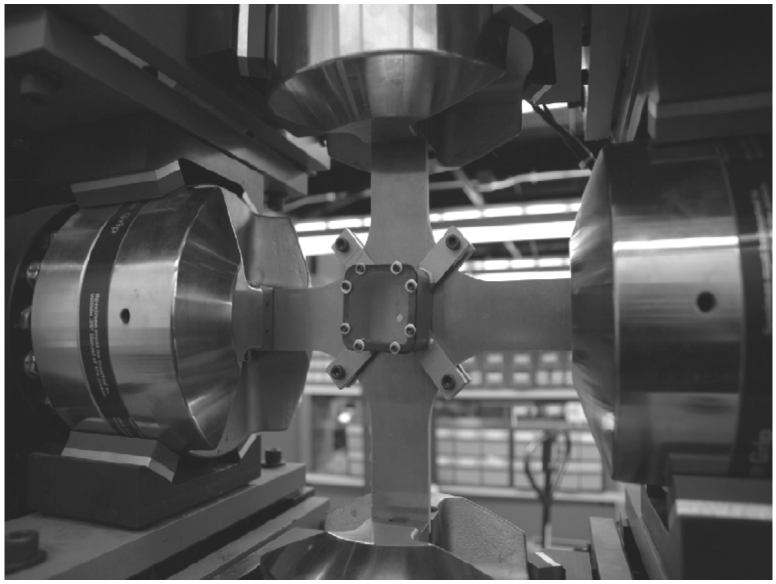

Figure 3.3: The Cruciform Specimen With Saltwater Chamber Attached to It.

Images of the results during the experiment were recorded with a PixeLINK camera. The images were taken after timed intervals to record the crack behaviors. The PixeLINK camera was used at a resolution of 3 mega pixels using an AF Micro Nikko 200 mm lens. When the crack grew to a length of approximately 20 mm the experiment was stopped. The resulting images were studied with uSCOPE software. The software measured the crack lengths using a resolution of 0.01 mm.

3.5 Finite Element Modeling

The stress intensity factor was calculated using Abaqus/CAE 6.10-1 for the test specimens, for both modes. The following assumptions applied:

1. The material was isotropic and homogeneous.
2. The mechanical properties of the aluminum alloy remained constant throughout the experiments (E=73 GPa, ν=0.33).

3. The center hole in all of the specimens had the same uniform shape with smooth edges.
4. The experimental specimens used did not have flaws and no cracks except for the cracks initiated from the pre-cracked notched hole.
5. The applied loads have no variation.

In Abaqus, a model was designed exactly according to the experimental specimens' dimensions. A sketch of pre-crack and notch locations were added to the model. The properties of the aluminum alloy 7075-T6 were assigned into the part. Next, the pre-crack direction were defined to the tip of the pre-crack with its prerequisite constraints. The experiments' dynamic loads and specimen constraints were input. After that, a mesh was produced for the each specimen.

A job was created and submitted after the mesh was completed. Each specimen was analyzed during the run of the job submmition. The computer results included the values for K_I, G and crack direction. The other cases have the exact same procedures, but with changing the lengths of the crack and the dynamic loads. Abaqus modeling procedure is available in Appendix A.

IV. Results and Discussion

4.1 Overview

As mentioned in the previous chapters, the fatigue crack growth behavior of specimens of 7075-T6 aluminum alloy was examined under in-plane biaxial loading in both air and saltwater (3.5% NaCl) environments with 0.5, 0, -0.5, and -1 biaxial stress ratio λ to study the difference between the positive and negative biaxiality and the effects of the negative biaxiality on crack propagation path and crack growth rate.

Section 4.2 in this section we are going to study the crack propagation direction for all specimens tested in air and saltwater environments. Then, section 4.3 will show and study the effects of the negative biaxiality on the crack growth rate in both air and saltwater environments. Finally, section 4.4 will present and study the microstructure results of the cracks surfaces. Table 4.1 shows a summary of the tests under fatigue loads with 0.5, 0, -0.5 and -1 biaxial stress ratio λ in air and saltwater environments.

Table 4.1: Summary of tests with 0.5, 0, -0.5, and -1 biaxial stress ratio λ in air and saltwater environments.

Environment	$R_{x,y}$	**λ**	**Frequency (Hz)**	**Total Initial ΔK ($MPa \cdot m^{1/2}$) (FEA)**
Air	0.5	0	10	4.026025
Air	0.5	0.5	10	3.368765
Air	0.5	-0.5	10	4.72659
Air	0.5	-1	10	5.48557
Saltwater	0.5	0	10	4.026025
Saltwater	0.5	0.5	10	3.34571
Saltwater	0.5	-0.5	10	4.72659
Saltwater	0.5	-1	10	5.48557

4.2 Crack Path

In uniaxial (λ = 0) experiment, the crack path looked the same for both air and saltwater environments. The crack growth at 90° angle to the direction of the load and it was collinear to the precrack and notch. The crack path did not change due to the absence of mode II stress intensity factor (K_{II} = 0) [25]. Figure 4.1 shows the crack path of a uniaxial specimen tested under cyclic load in air and saltwater.

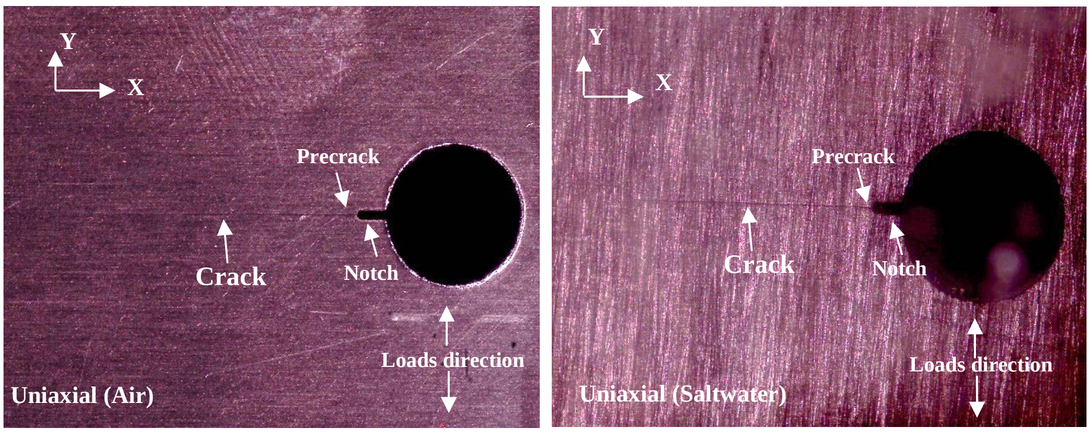

Figure 4.1: The Crack Path of an AA 7075-T6 Uniaxial Specimen Tested under Cyclic Load in Air and Saltwater Environments.

In biaxial (λ = 0.5, -0.5, -1) experiments, the crack looked the same for all biaxility ratios in both air and saltwater environments. The crack growth at 90° angle to the load applied in y-direction and it was collinear to the precrack and notch as in the case of the uniaxial fatigue. Figure 4.2 shows the crack path of an AA 7075-T6 biaxial specimen tested under cyclic load in air environment.

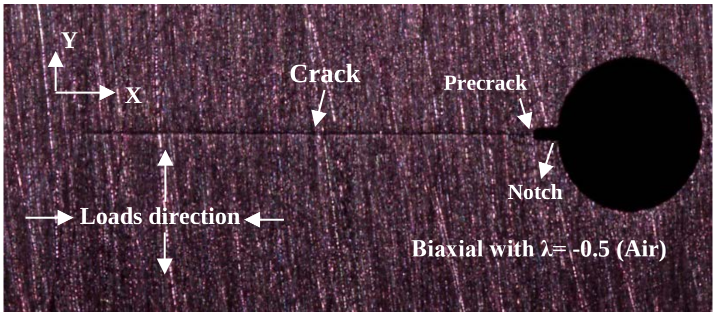

Figure 4.2: The Crack Path of an AA 7075-T6 Biaxial Specimen Tested under Cyclic Load in Air Environment.

The crack stayed collinear up to the failure of the specimens and didn't change its path as it propagated. Therefore, we could conclude the same explanation as the uniaxial experiment from the collinear path of the crack in the biaxial test which is the nonexistence of the mode II stress intensity factor (K_{II} = 0). This conclusion can be verified analytically using equation (2.36) and also, from the finite element analysis. Figure 4.3 shows the direction of crack propagation for this case.

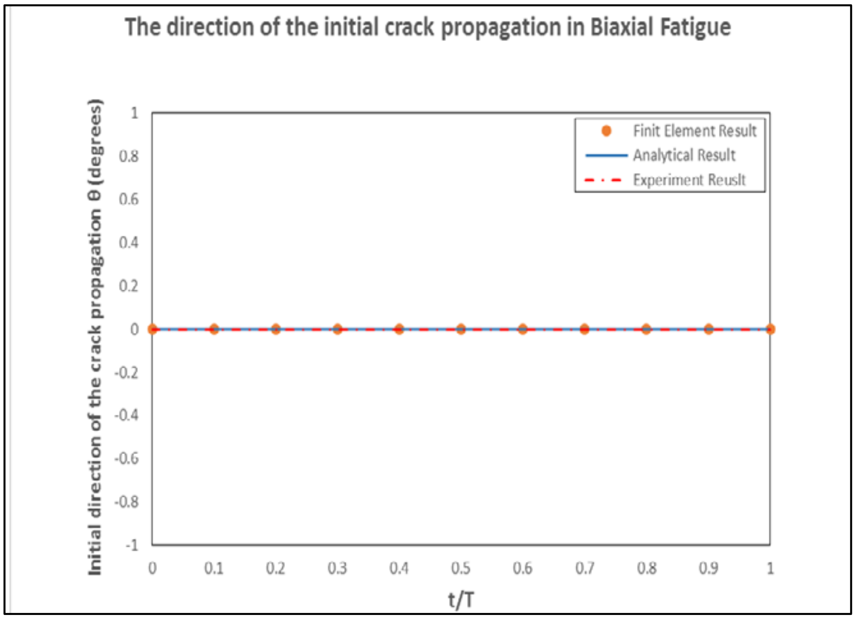

Figure 4.3: The Direction of the Initial Crack Path of an AA 7075-T6 Biaxial Specimen under Fatigue Load in Air and Saltwater Environments Using Analytical, Finite Element and Experimental Methods.

4.3 Crack Growth Rate

Crack growth rates (da/dN) were calculated from the measured crack length and its corresponding number of cycles relationship. It is common to define fatigue crack growth behavior by the relationship between crack growth rate (da/dN) and the crack driving force. After that, these were correlated with the crack driving forces to explain the fatigue crack growth behavior. Mode I stress intensity factor range (ΔK_I) usually states the crack driving force, and that's when the crack is collinear to the precrack

4.3.1 Crack Growth Rate of Uniaxial Specimen λ = 0 in Air and Saltwater Environments

In this case, the fatigue load was applied in Y-direction only. The maximum load was 12000 N and the minimum load was 6000 N. Figure 4.4 shows the load applied versus the time. The crack length versus number of cycles for λ = 0 specimen in air and saltwater environments can be seen in Figure 4.5.

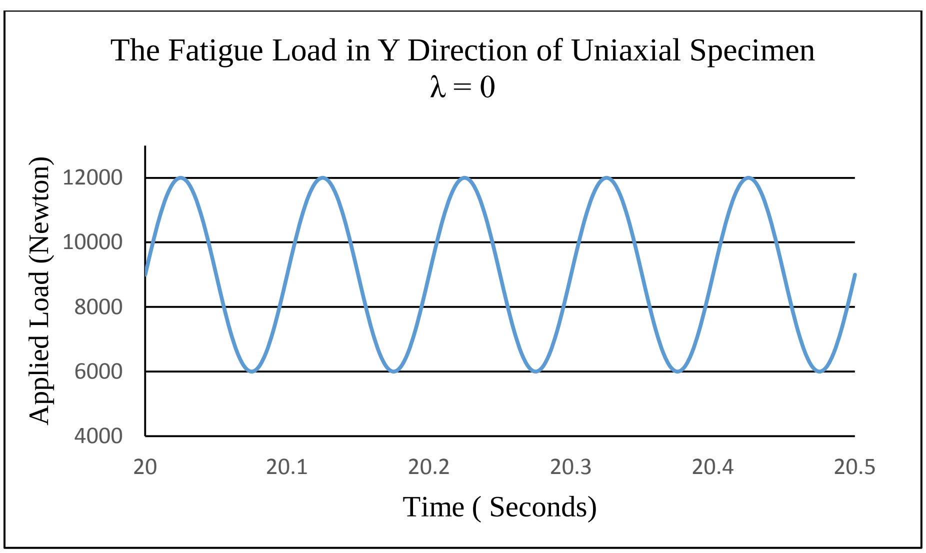

Figure 4.4: The Applied Loads of Specimen λ = 0 in Air and Saltwater Environments.

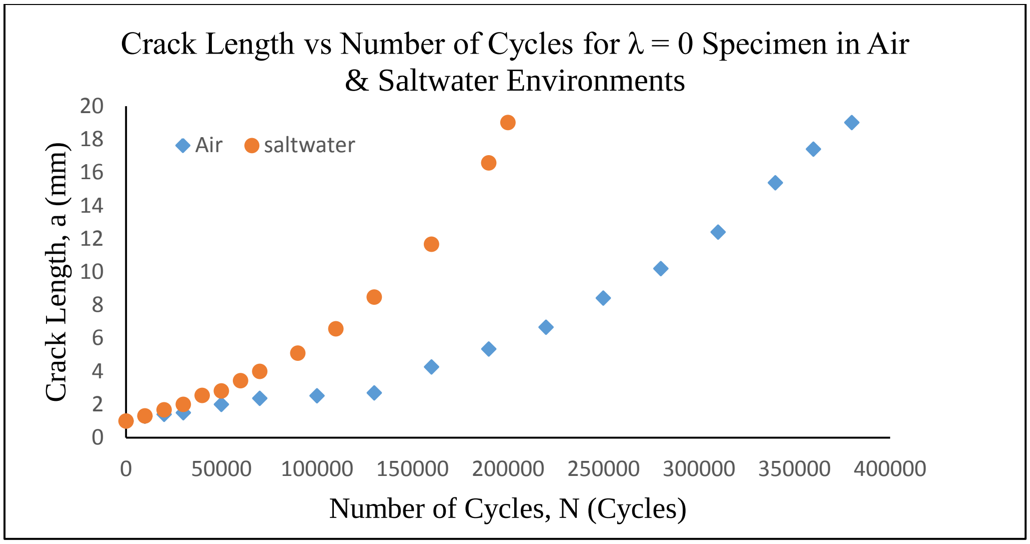

Figure 4.5: Crack Length Versus Number of Cycles for λ = 0 Specimen in Air & Saltwater Environments.

Figure 4.6 shows the crack growth behavior for uniaxial tests λ = 0 in air and saltwater environments by looking into the relationship between the crack growth rate (da/dN) and the stress intensity factor (ΔK). In both environments, seem to have the same crack growth rate versus stress intensity factor curve. In other words, as (ΔK) increases, the (da/dN) increases too but in saltwater environment the curve of crack growth rate versus the stress intensity factor (ΔK) is higher than the air environment by 36%.

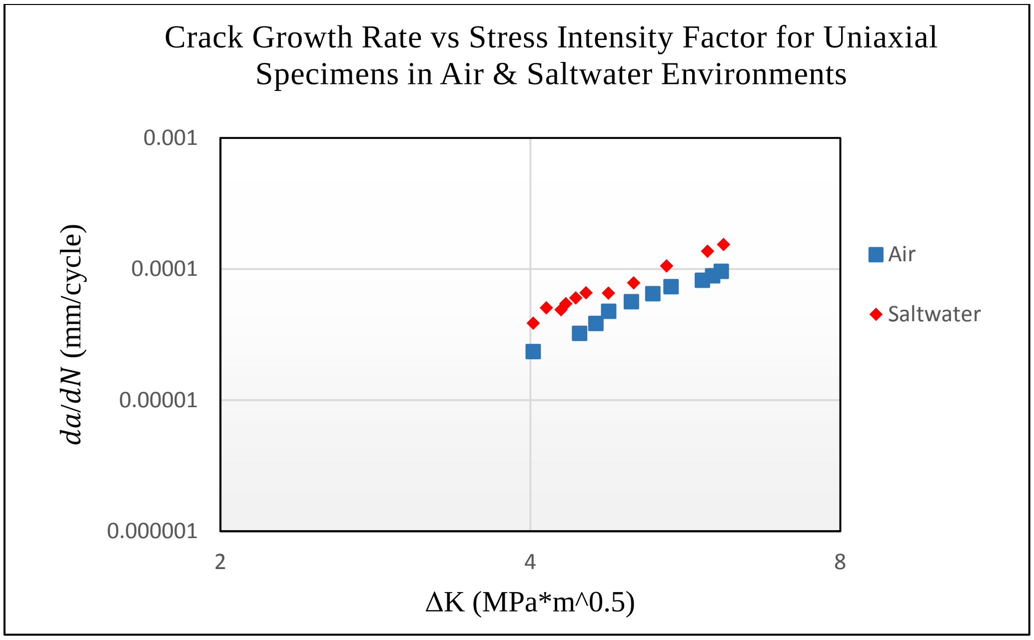

Figure 4.6: Crack Growth Rate versus Stress Intensity Factor for Uniaxial Specimens in Air and Saltwater Environments.

4.3.2 Crack Growth Rate of Biaxial Specimen λ = 0.5 in Air and Saltwater Environments

Figure 4.7 shows the applied load on biaxial specimen with λ = 0.5 for both air and saltwater environments. The maximum and minimum loads in Y-direction were 12000 N and 6000 N respectively. There for, the maximum and minimum loads on X-direction were 6000 N and 3000 N respectively. Figure 4.8 shows the crack length versus number of cycles for biaxial specimen λ = 0.5 for both air and saltwater environments. The crack propagates in the saltwater environment faster than the air environment.

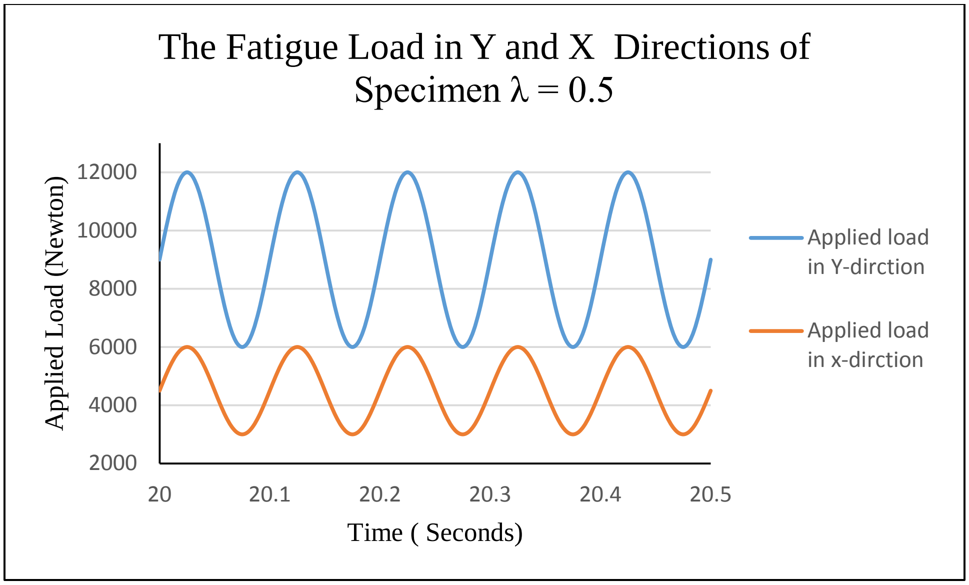

Figure 4.7: The Applied Loads of Specimen λ = 0.5 in Air and Saltwater Environments.

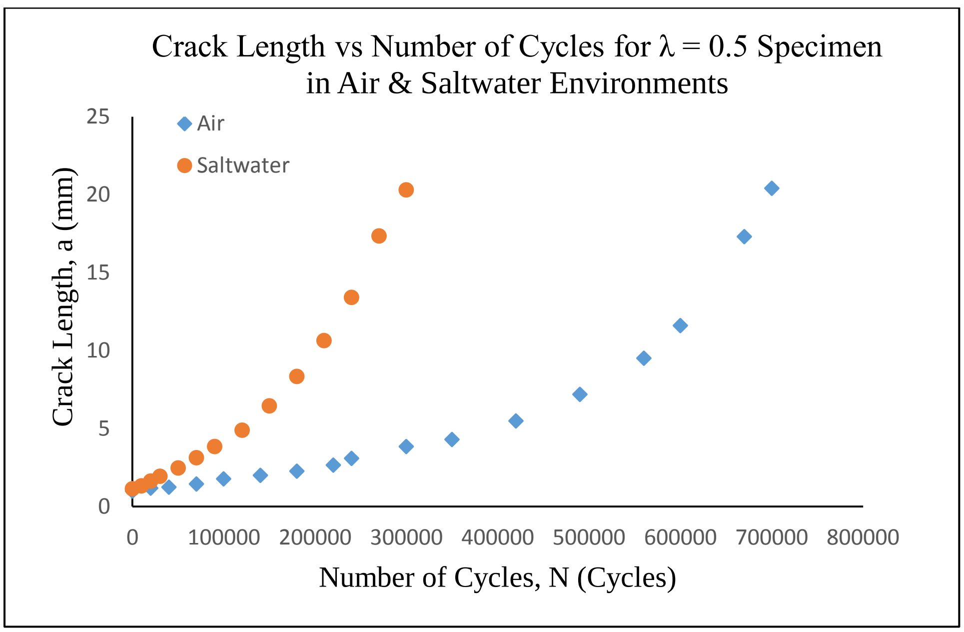

Figure 4.8: Crack Length versus Number of Cycles for λ = 0.5 Specimen in Air & Saltwater Environments.

Figure 4.9 shows the crack growth behavior for biaxial tests λ = 0.5 in air and saltwater environments by looking into the relationship between the crack growth rate (da/dN) and the stress intensity factor (ΔK). They seem to have the same crack growth rate versus stress intensity factor curve as stress intensity factor increases, the crack growth rate increases too but in saltwater environment the curve is higher than the air environment, which means that corrosion accelerates the crack growth rate.

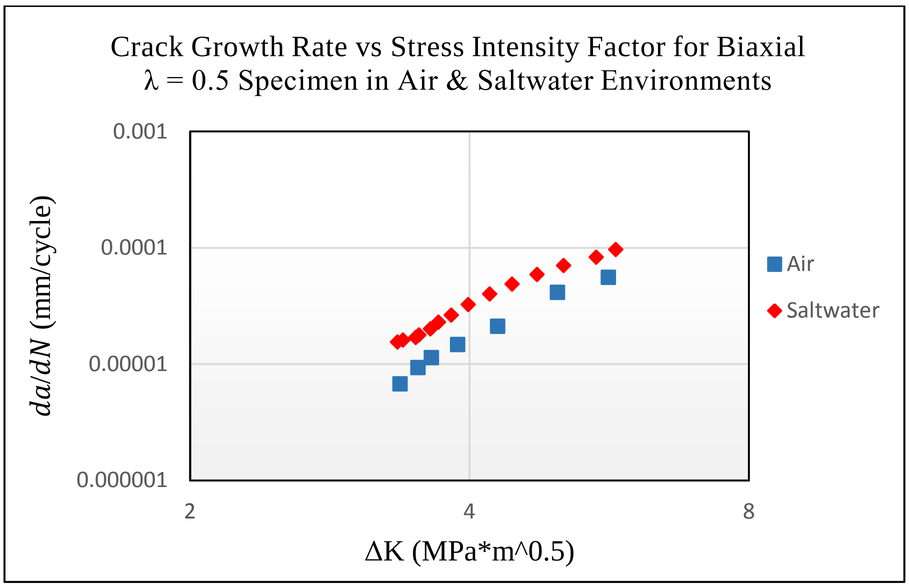

Figure 4.9: Crack Growth Rate versus Stress Intensity Factor for Biaxial Specimen λ = 0.5 in Air and Saltwater Environments.

4.3.3 Crack Growth Rate of Negative Biaxial Specimen λ = -0.5 in Air and Saltwater Environments

In this case, a tensile load was applied in Y-direction and a compression load in X-direction simultaneously. The maximum and minimum loads on Y-direction were 12000 N and 6000 N respectively. There for, the maximum and minimum loads on X-direction were 6000 N (compression) and 3000 N (compression) respectively, Figure 4.10.

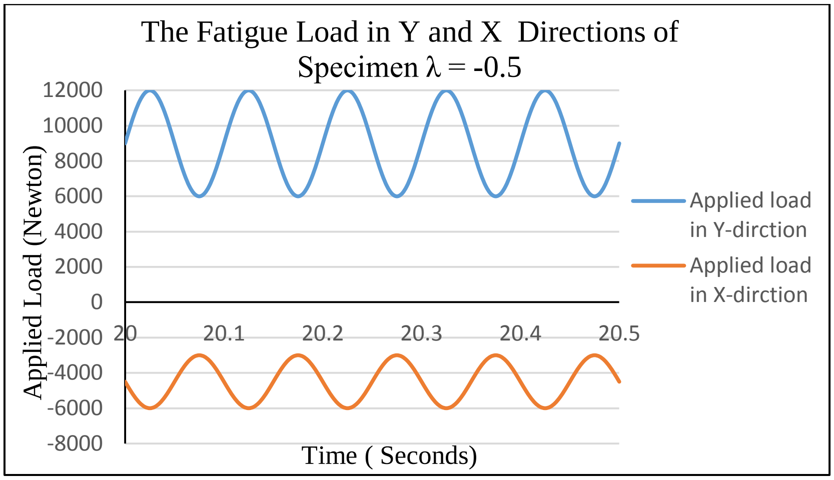

Figure 4.10: The Applied Loads of Specimen λ = -0.5 in Air and Saltwater Environments.

The relationship between the crack length and the number of cycles for the negative biaxiality case λ = -0.5, Figure 4.11. It was also observed that in saltwater environment the crack propagates faster than air environment due to corrosion atmosphere, which means that the crack needed less number of cycles to reach failure in saltwater environment comparing to air environment.

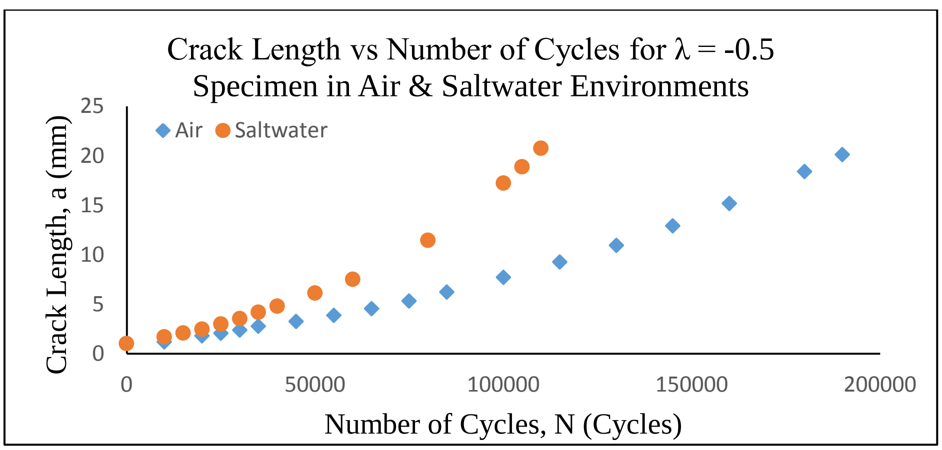

Figure 4.11: Crack Length versus Number of Cycles for λ = -0.5 Specimen in Air & Saltwater Environments.

Figure 4.12 shows the relationships between crack growth rates (da/dN) and stress intensity factor (ΔK) for negative biaxial specimen λ = -0.5. The curve of saltwater environment was higher than air environment, which shows that with corrosion the crack propagates faster.

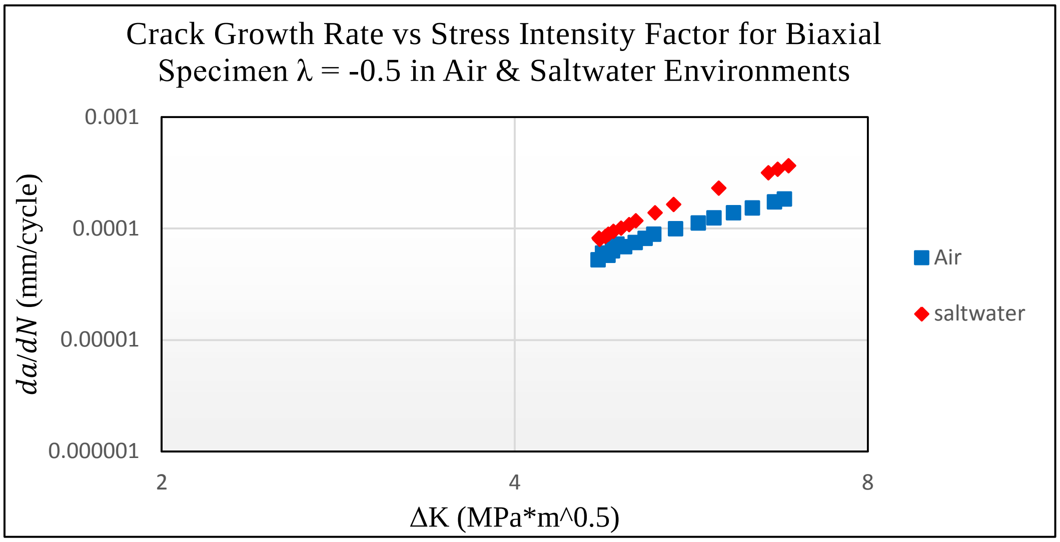

Figure 4.12: Crack Growth Rate versus Stress Intensity Factor for Negative Biaxial Specimen λ = -0.5 in Air and Saltwater Environments.

4.3.4 Crack Growth Rate of Negative Biaxial Specimens λ = -1 in Air and Saltwater Environments

In this case, the specimen experienced a tensile load in Y-direction and a compression load in X-direction with the same magnitude. The maximum load was 12000 N and the minimum load was 6000 N, Figure 4.13. The relationship between the cracks' length and the number of cycles for this case (λ = -1) is shown in Figure 4.14. As expected, the crack length increases as the number of cycles increases. In saltwater environment, the crack needed less number of cycles, Figure 4.14.

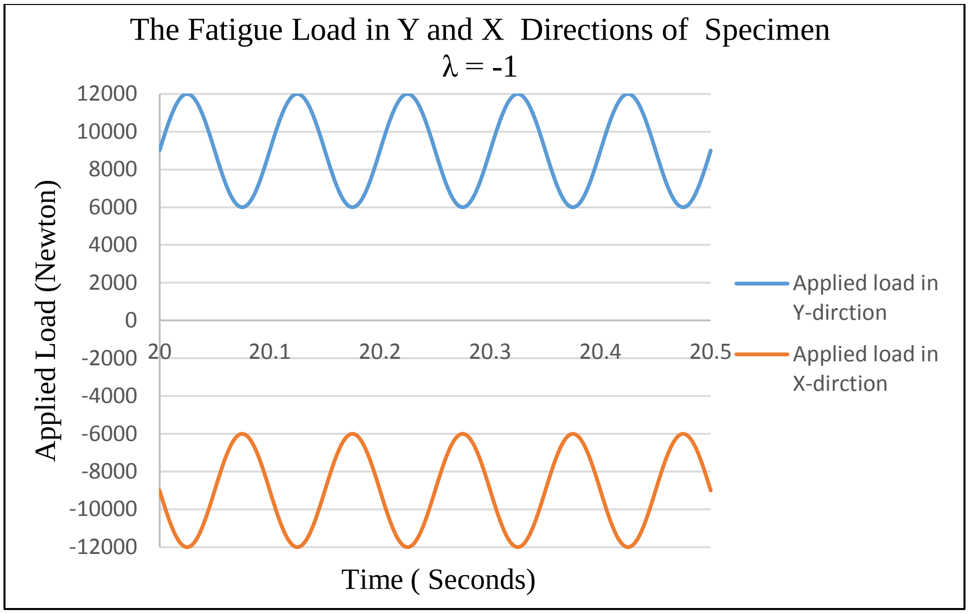

Figure 4.13: The Applied Loads of Specimen λ = -1 in Air and Saltwater Environments.

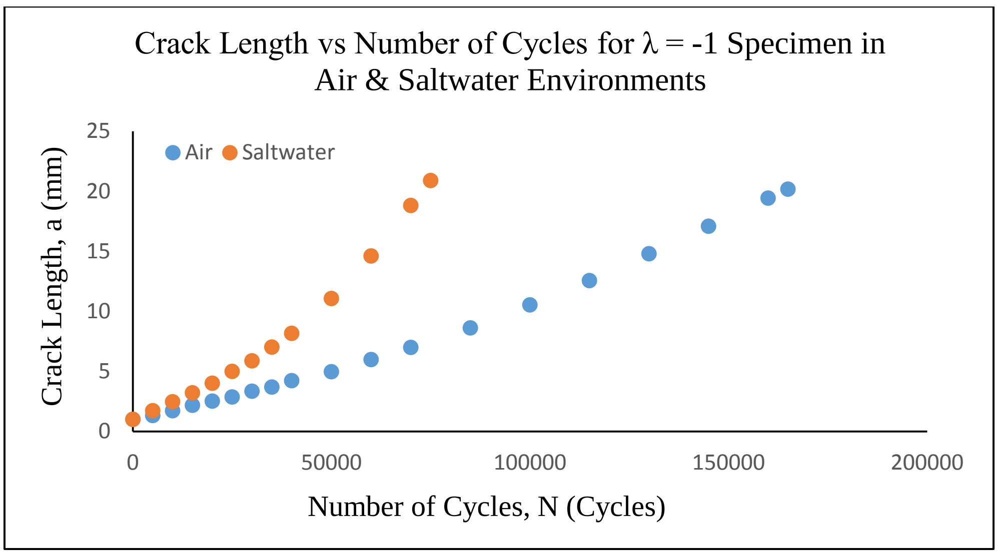

Figure 4.14: Crack Length versus Number of Cycles for λ = -1 Specimen in Air & Saltwater Environments.

Figure 4.15 shows the relationships between crack growth rates (da/dN) and stress intensity factor (ΔK) for negative biaxial specimen λ = -1. The curve of saltwater environment was higher than air environment, which shows the crack grows faster in saltwater environment due to the existing of corrosion.

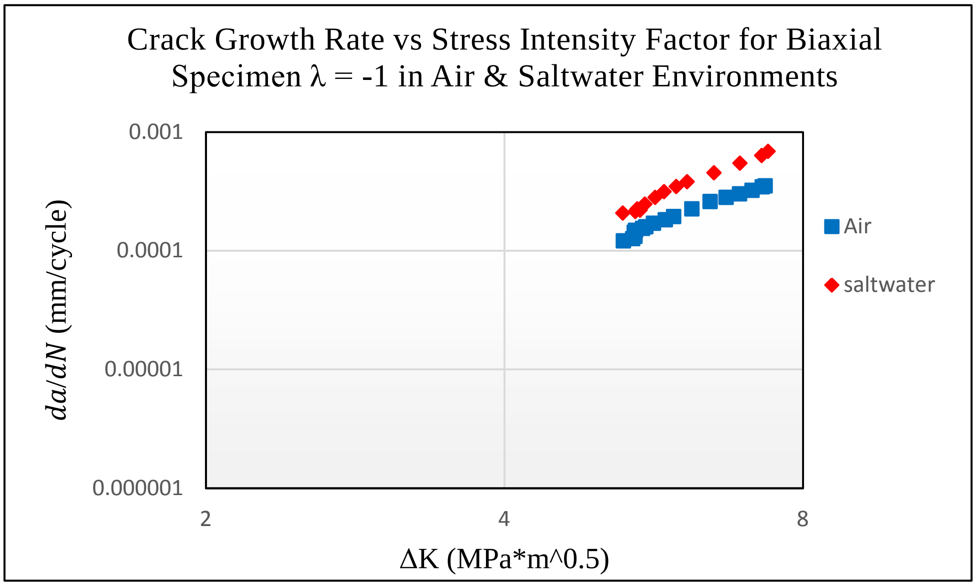

Figure 4.15: Crack Growth Rate versus Stress Intensity Factor for Negative Biaxial Specimen λ = -1 in Air and Saltwater Environments.

4.3.5 Crack Growth Rate of All Specimens in Air and Saltwater Environments

Now, for purpose of comprehension and correlation, all tests were plotted in figures together to give a superior look to the impacts of changing the biaxial ratio λ on the crack growth rate versus the stress intensity factor. Figure 4.16 delineates the relationship between the crack length and the number of cycles for all tests in air environment. It was observed that when biaxial ratio λ decreased the crack required less number of cycles. In saltwater environment, appears to have the same result, which is as the biaxial ratio λ decreased the crack required less number of cycle to fail, Figure 4.17.

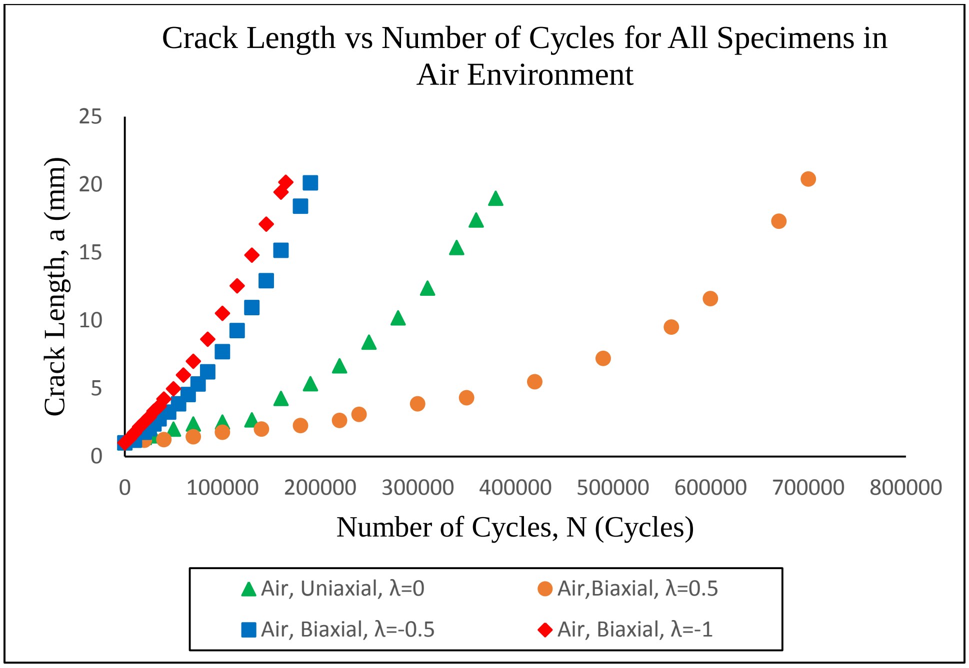

Figure 4.16: Crack Length versus Number of Cycles for All Specimens in Air Environment.

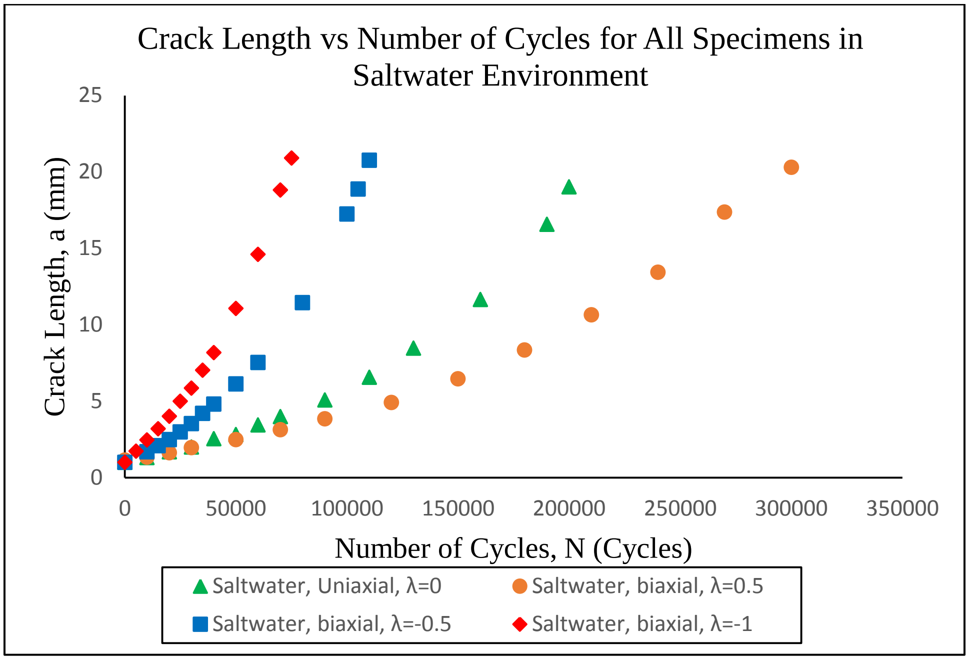

Figure 4.17: Crack Length versus Number of Cycles for All Specimens in Saltwater Environment.

Figure 4.18 shows the crack growth rates (da/dN) versus stress intensity factor (ΔK) for all specimens in air environment. It was observed that the curve located higher as the biaxial ratio decreased. This means that crack propagated faster when the biaxial ratio decreased. Also, the stress intensity factor (ΔK) greatly increased at same crack length when the biaxial ratio decreased. Figure 4.19 shows that the curves of (da/dN) versus (ΔK) of all experiments tested in saltwater environment. It shows the same tendency comparing to the air environment. As λ decreased, the curve moves upper and ΔK sufficiently increased at the same crack length.

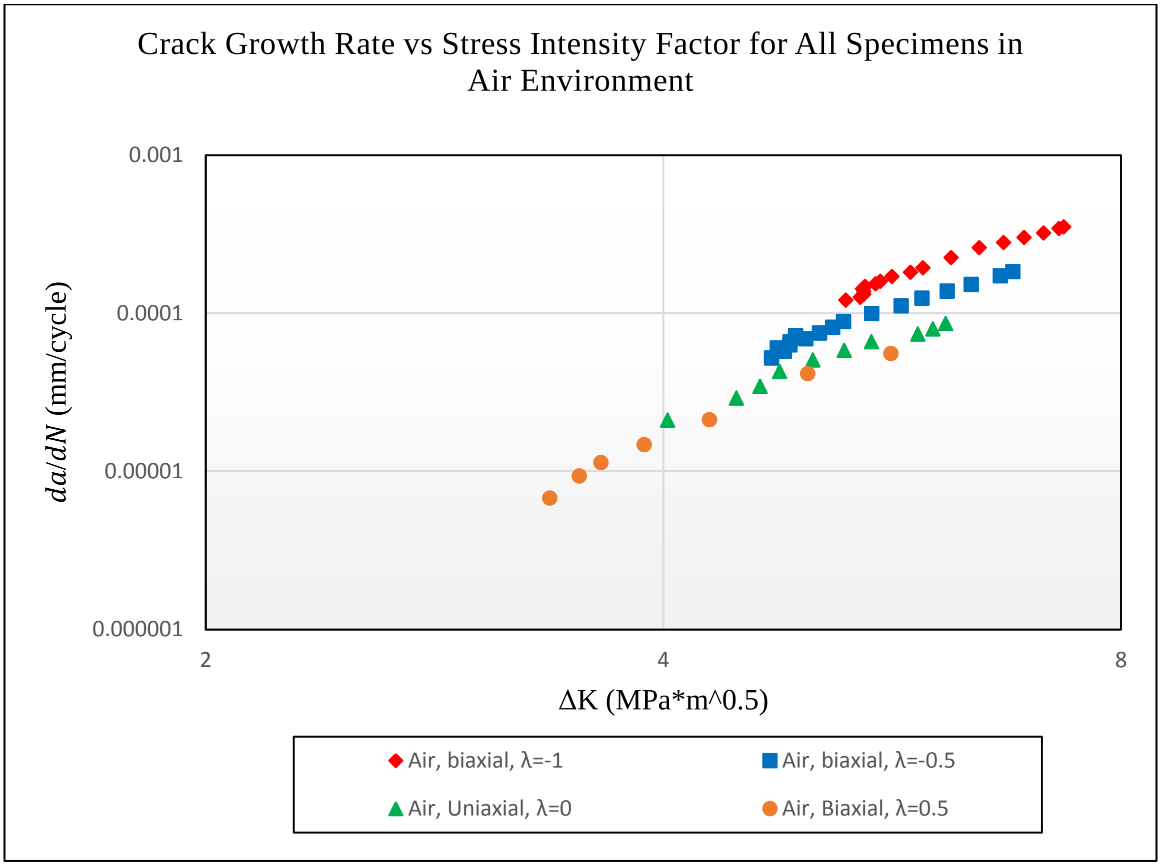

Figure 4.18: Crack Growth Rate versus Stress Intensity Factor for All Specimens in Air Environment.

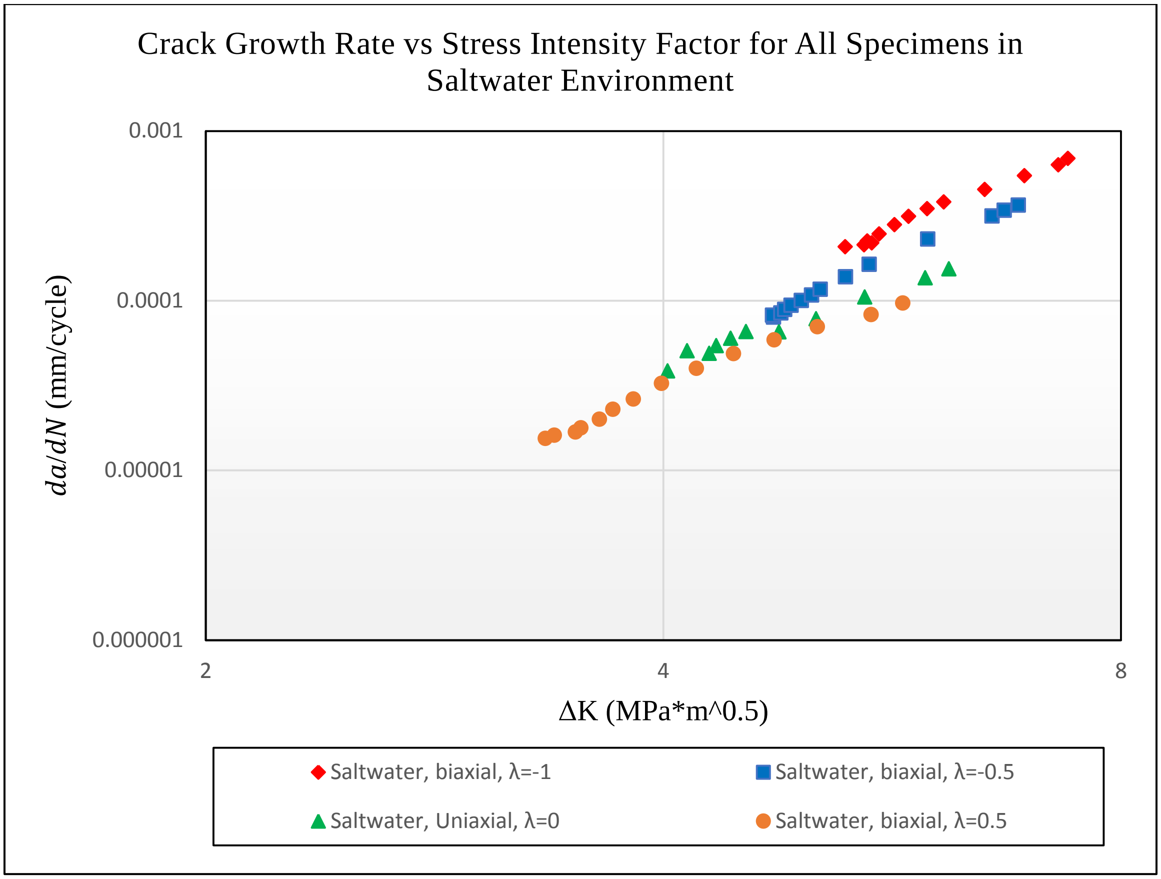

Figure 4.19: Crack Growth Rate versus Stress Intensity Factor for All Specimens in Saltwater Environment.

4.4 Fractography

After performing the experiments, the tested specimens were cut on small sections with fragments of the fracture surfaces using a band saw. This allowed the crack surfaces to be examined using a Scanning Electron Microscope (SEM). Fracture surface for the specimen tested at λ=-1 was the smoothest surface. The smoothness keeps decreasing as the biaxial ratio increases, Figure 4.20.

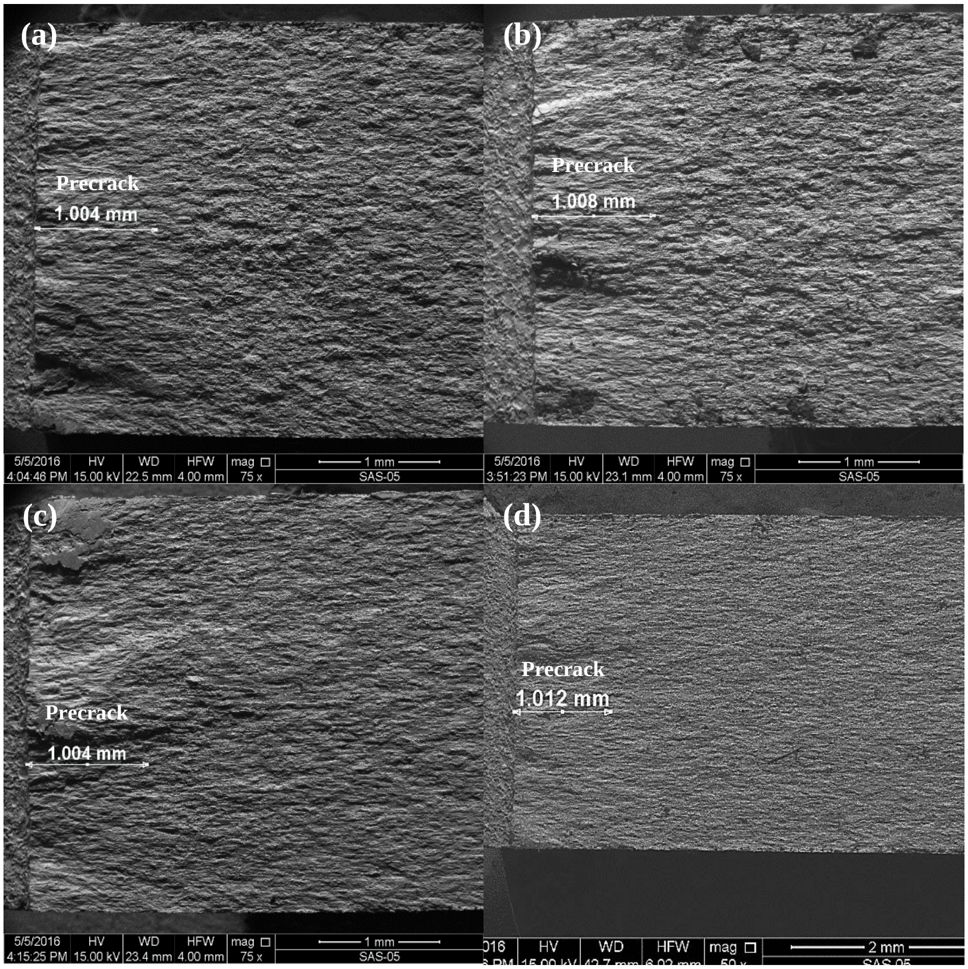

Figure 4.20: SEM Images of Fracture Surfaces for Different Biaxial Cases in Air Environment: (a) biaxial (λ= 0.5), (b) uniaxial (λ= 0), (c) biaxial (λ= -0.5), (d) biaxial (λ= -1).

The uniaxial (λ= 0) and the negative biaxiality (λ= -0.5, -1) have a planar slip microstructural feature. In case of positive biaxiality (λ= 0.5), the fracture surface has a combination of planar and wavy slip microstructural features. See Appendix C.

V. Conclusions and Recommendations

5.1 Conclusions

This thesis presents the results of a study to quantify the effects of biaxial loading on fatigue crack behavior in both air and saltwater (3.5% NaCl) environments from pre-cracked notched circular hole in a 7075-T6 cruciform specimen using a fracture mechanics approach. With stress ratio of R = 0.5, the crack growth behavior was investigated under in-plane biaxial tension-tension and compression-tension fatigue with 0.5, 0, -0.5, and -1 biaxial stress ratio λ. This research presents and documents the details of these experiments which can be useful to understand the concept of corrosion fatigue and overcome this mode of failure in the real applications. The following conclusions can be drawn from this study:

1. A single crack propagates collinear to the precrack and notch for negative biaxial and uniaxial fatigue.
2. The crack required less number of cycles to fail in saltwater environment, than in ambient air environment. The number of cycles in corrosion environment decreases on 57%. The number of cycles decreases when the biaxial ratio decreases.
3. The specimens tested with a negative biaxiality have a higher crack growth rate than a positive biaxiality and uniaxial loading. This happens due to the effect of Poisson's ratio. When the specimen is compressed in x-direction, it tends to expand in y-direction (i.e. perpendicular to the direction of compression).

4. At a given crack length, the stress intensity factor (ΔK) at the crack tip greatly increased as the biaxial ratio decreased.

5.2 Recommendations

More testing on the fatigue crack growth from cracks initiated from a notched circular hole in air and saltwater environment in AA 7075-T6 should be conducted due to the variability that is inherent in materials testing. To simulate real life boundary conditions, further analysis could be done for the negative biaxiality such as:

1. Different angles of the crack.
2. Multiple cracks.

Appendix A: Finite Element Method (FEA)

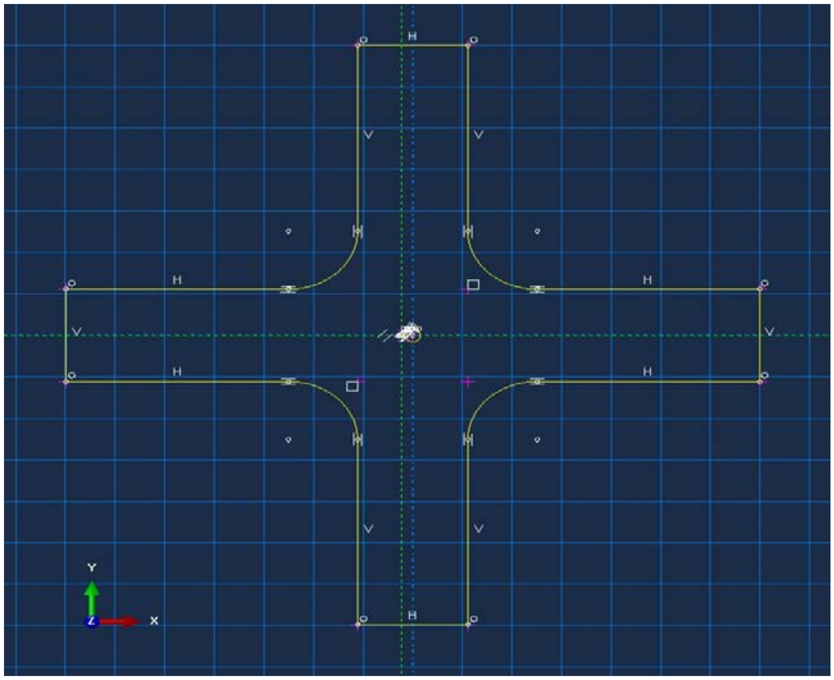

Figure A.1: Sketch of the Specimen in Abaqus Program.

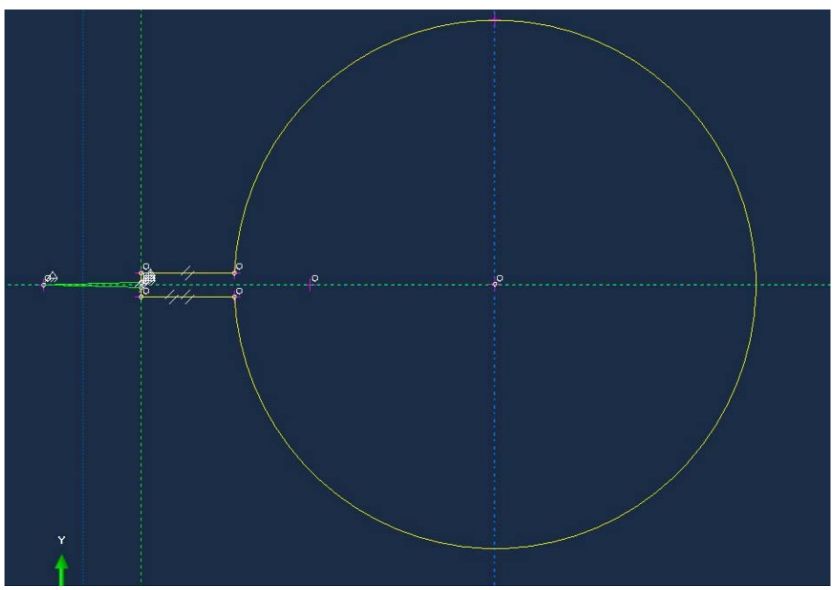

Figure A.2: Sketch of the Hole, Notch and the Precrack in Abaqus Program.

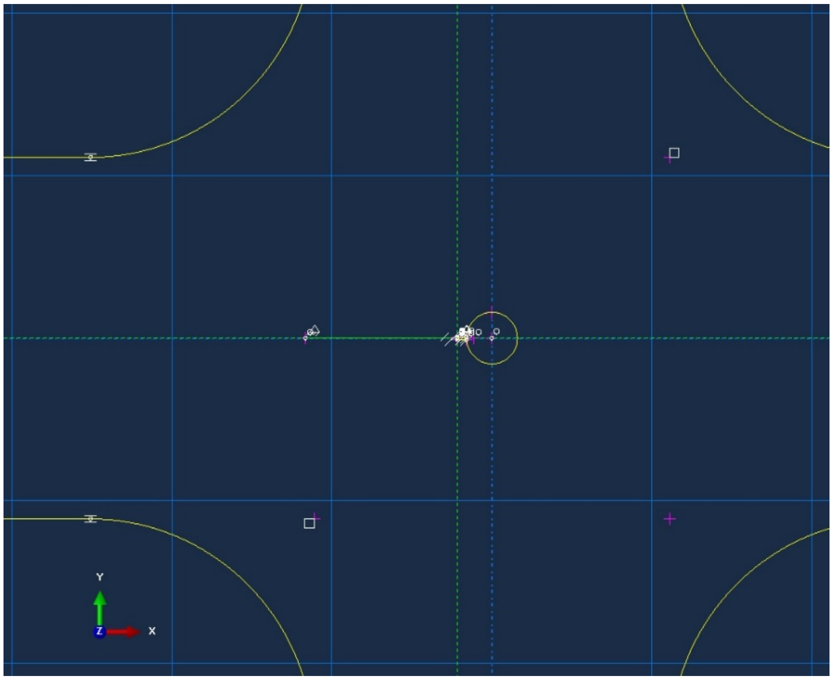

Figure A.3: Sketch of the Hole, Notch and the Crack in Abaqus Program.

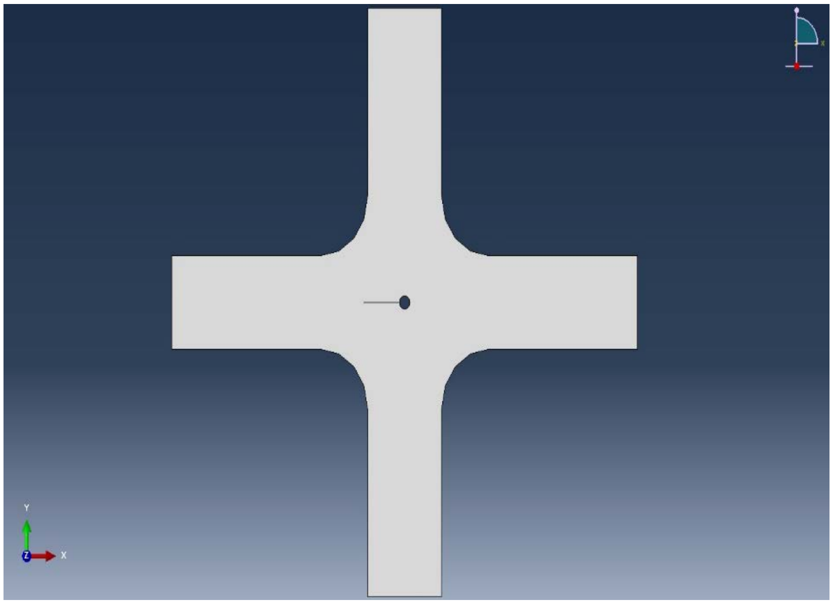

Figure A.4: The Whole Part of the Specimen in Abaqus Program with the Crack.

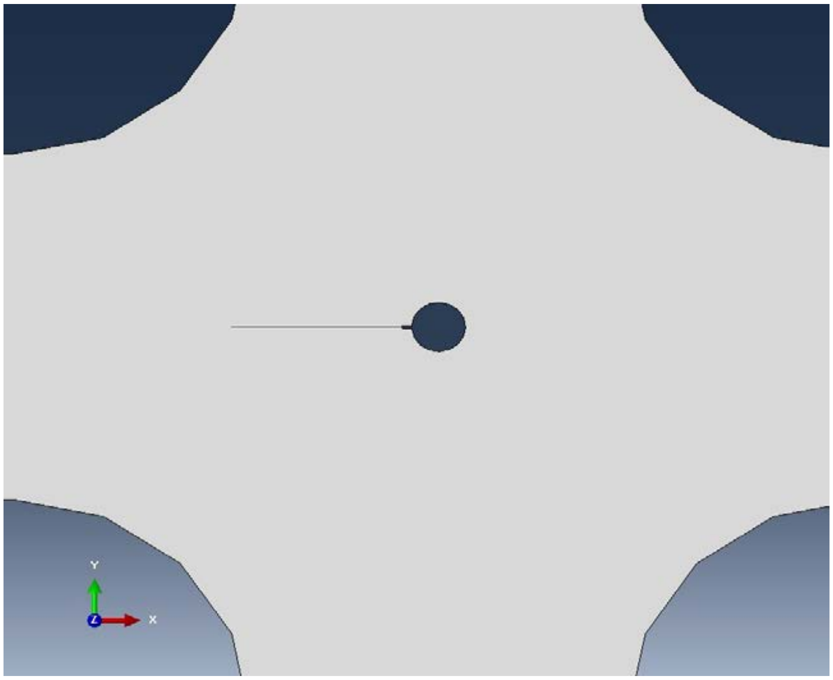

Figure A.5: A Closer Look to the Hole, Notch, and the Crack in Abaqus Program.

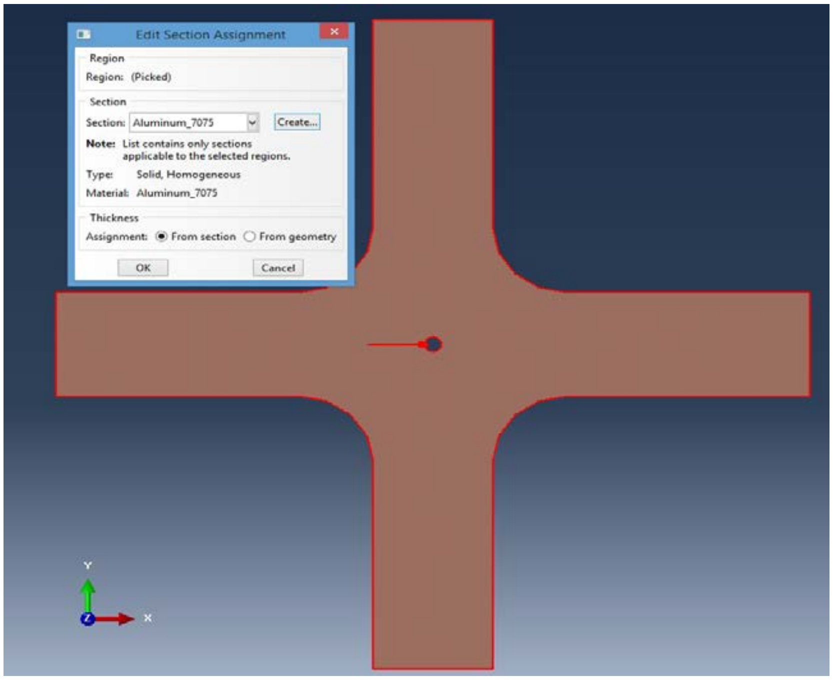

Figure A.6: Assigning the Material Type which is Aluminum Alloy 7075-T6 to the Specimen.

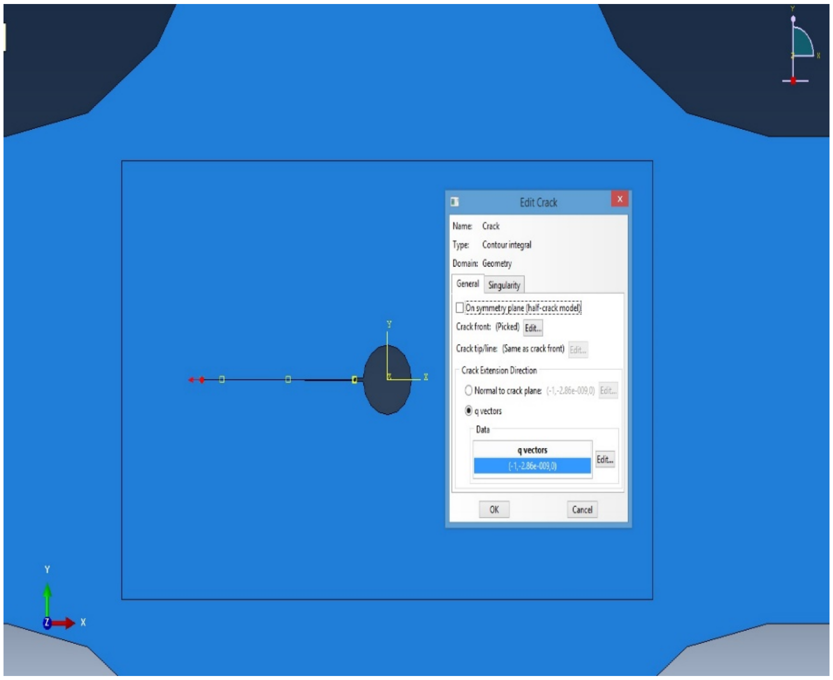

Figure A.7: Specifying the Location and the Direction of the Crack-tip.

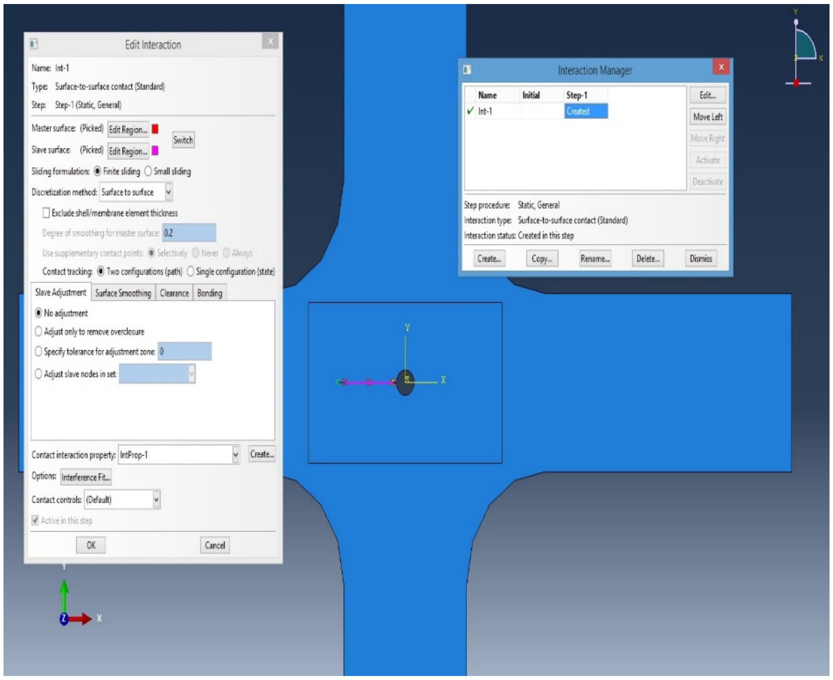

Figure A.8: Assigning the Masters' and the Slaves' Surfaces.

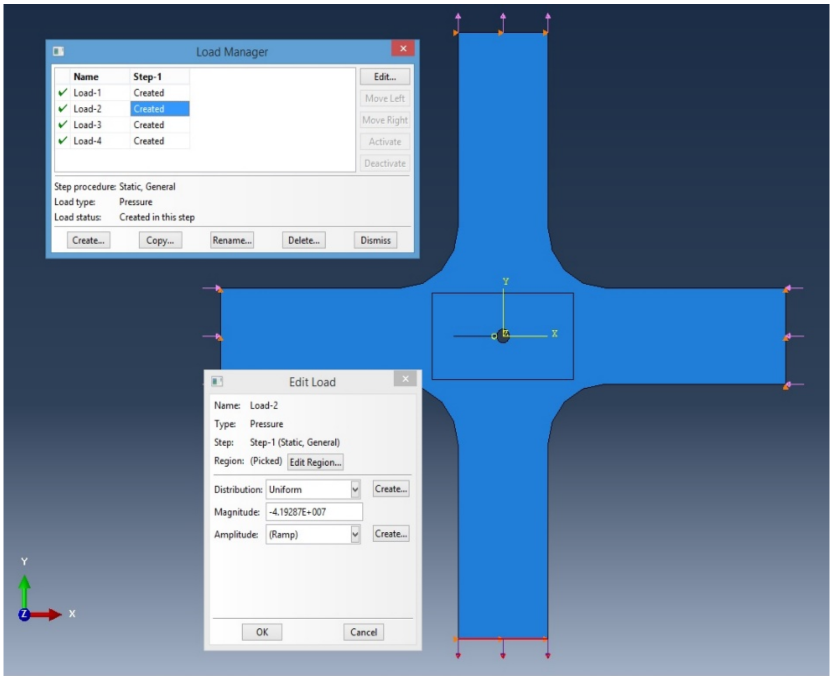

Figure A.9: Specifying the Loads to the Arms of the Specimen.

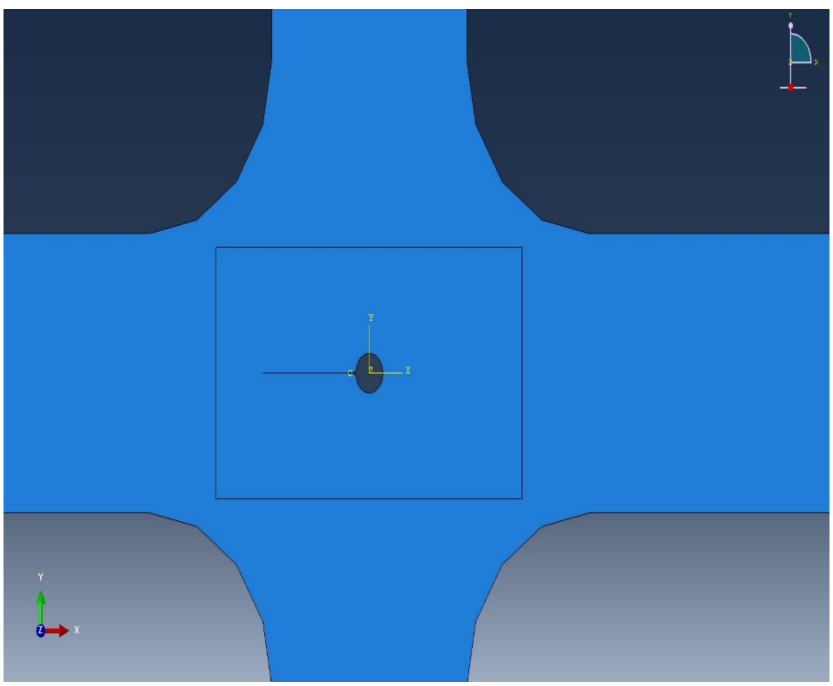

Figure A.10: Generating Partition for High Density Mesh in Order to Improve the Accuracy of the Results.

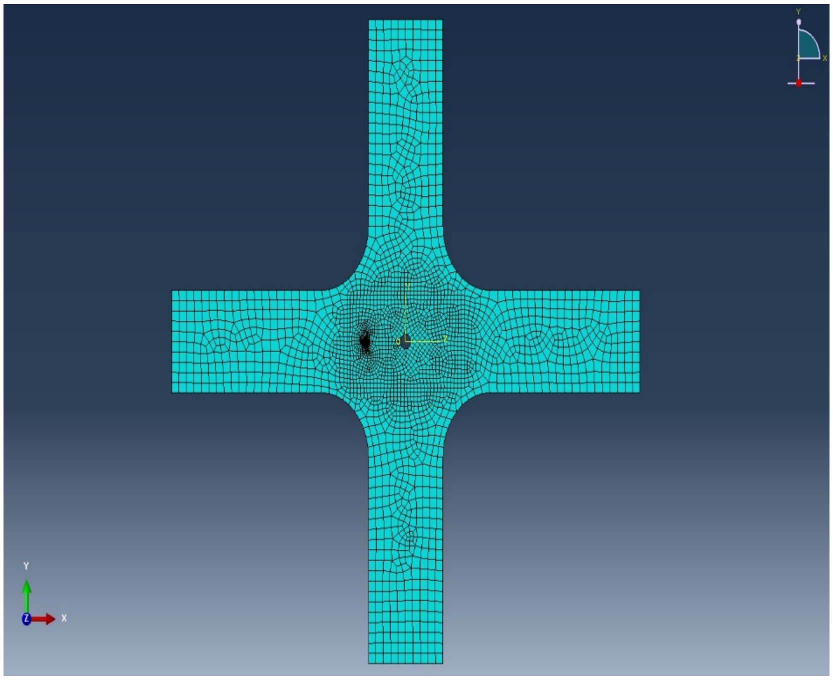

Figure A.11: Mesh of the Specimen in Abaqus Program.

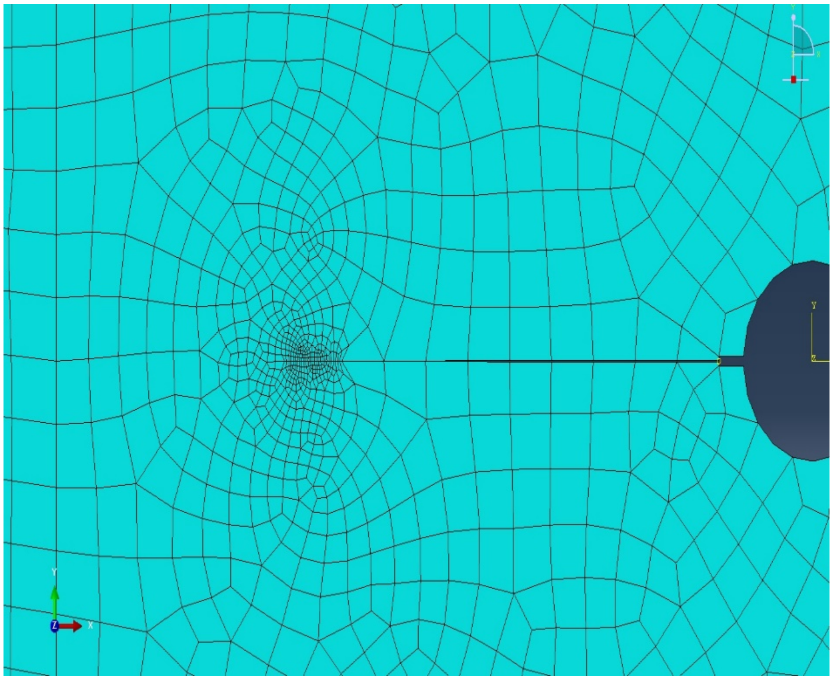

Figure A.12: A Closer View of the Mesh at the Crack-Tip.

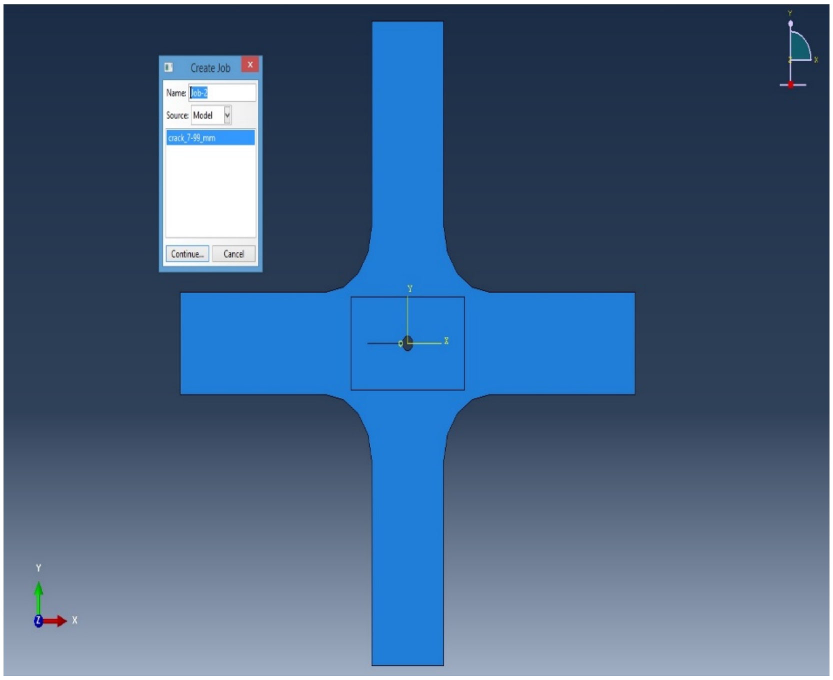

Figure A.13: Creating a Job for Submition in Abaqus Program.

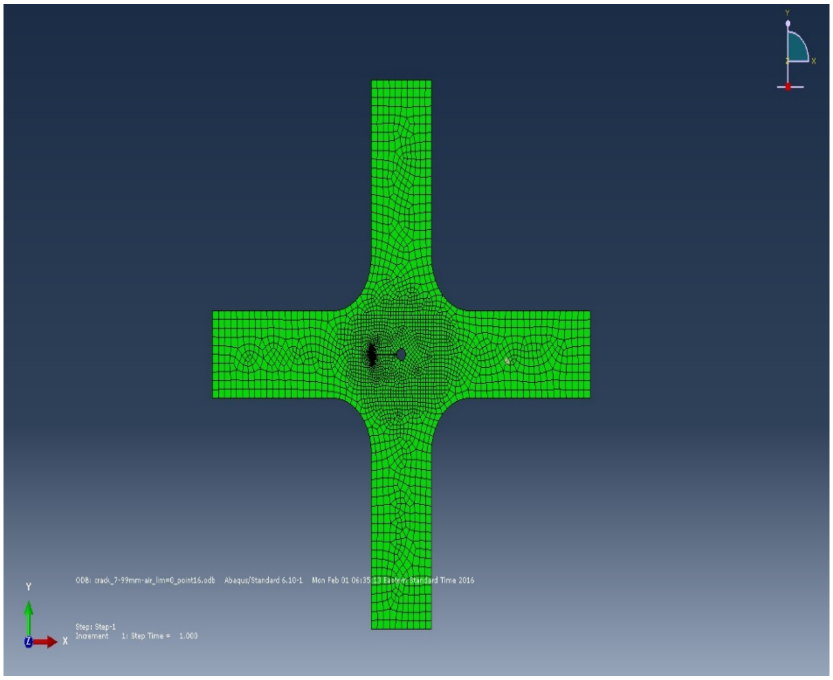

Figure A.14: Undeformed Shape of the Specimen After Job Submittion.

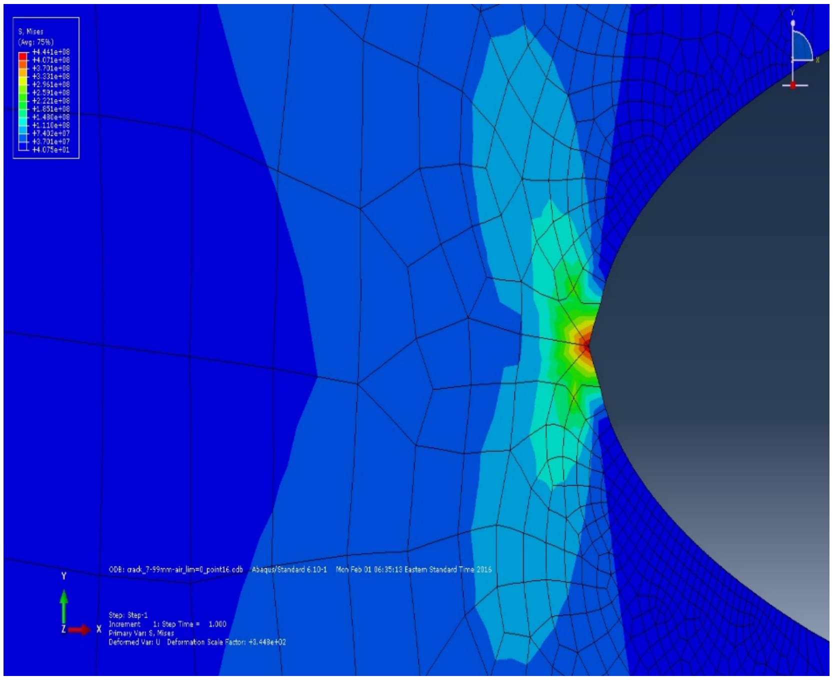

Figure A.15: The Stresses at the Crack-tip After Simulation.

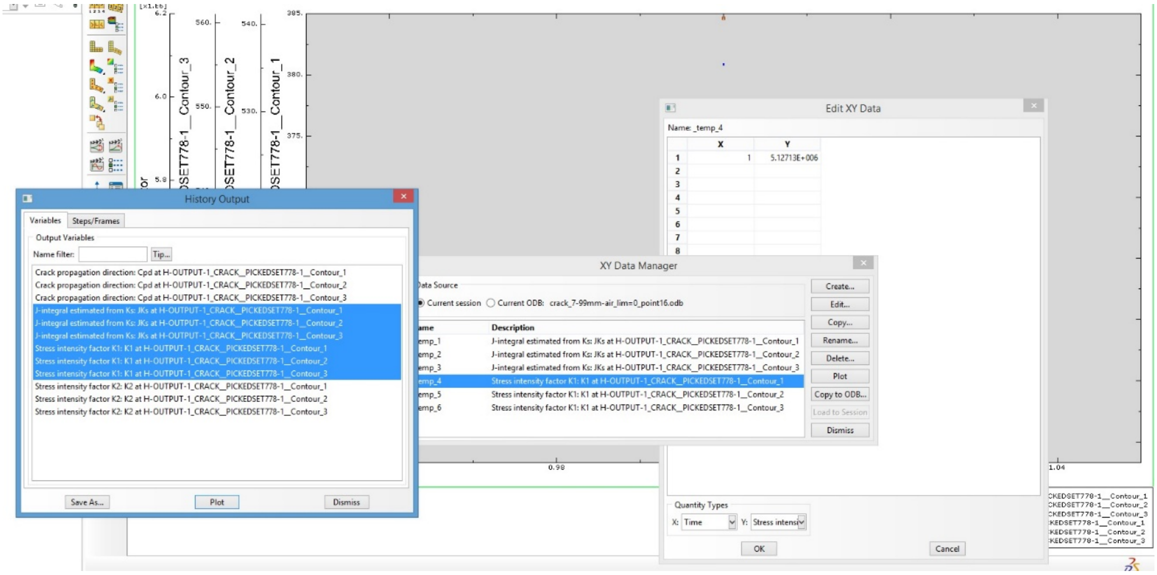

Figure A.16: Results After Finishing the Calculations in Abaqus Program.

Table A.1: ΔK for all biaxial ratios at 10 mm crack length.

Biaxial Ratio (λ)	**stress intensity factor (ΔK) (MPa*m^0.5)**
0.5	4.6
0	5.17
-0.5	5.72
-1	6.3

Appendix B: Pictures of the Cracks at Different Biaxiality ratio, Conditions and Environments.

Figure B.1: Crack Shape for λ=0 at 220,000 Cycles in Air Environment.

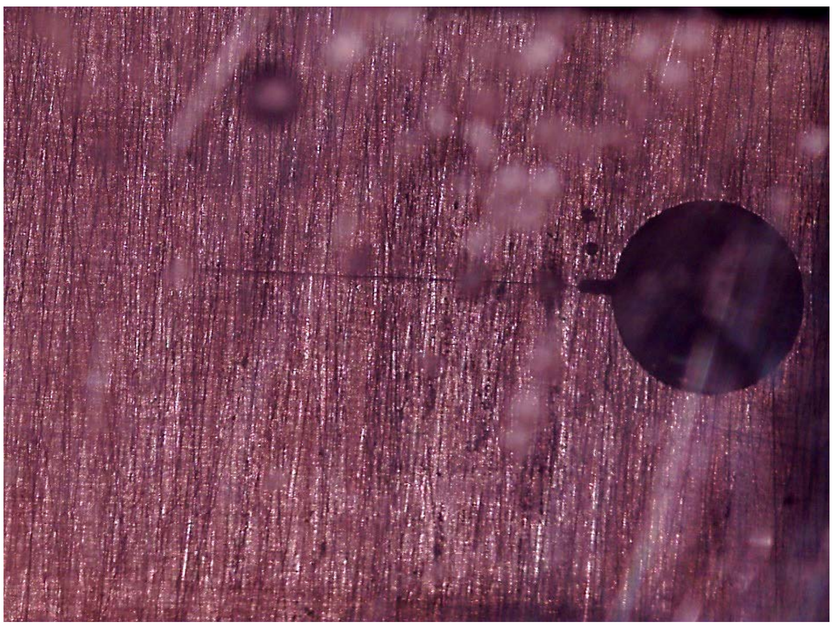

Figure B.2: Crack Shape for λ=0 at 160,000 Cycles in Saltwater Environment.

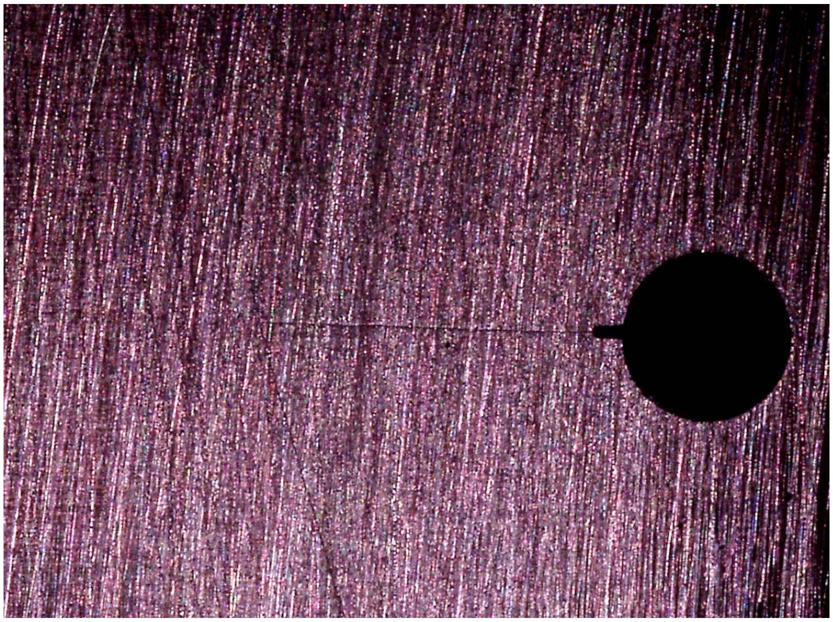

Figure B.3: Crack Shape for λ=0.5 at 600,000 Cycles in Air Environment.

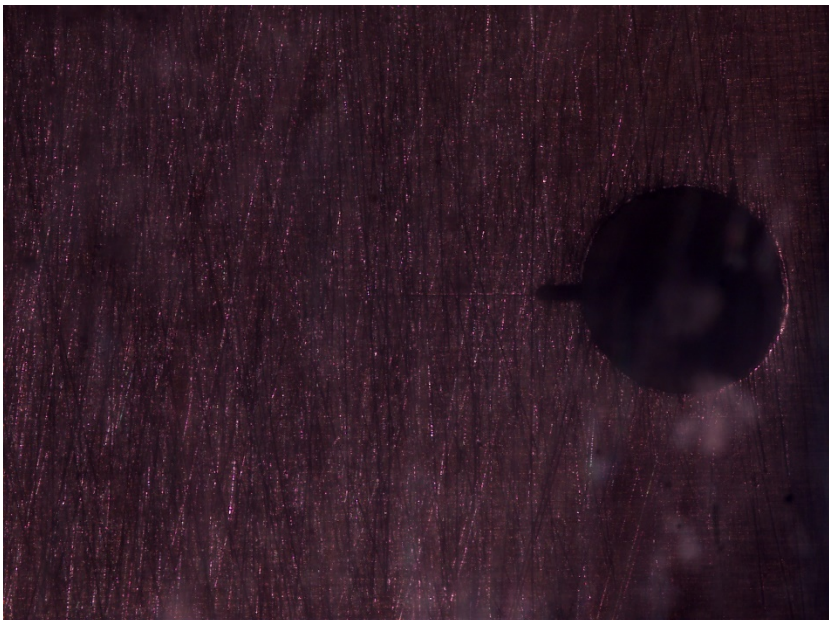

Figure B.4: Crack Shape for λ=0.5 at 120,000 Cycles in Saltwater Environment.

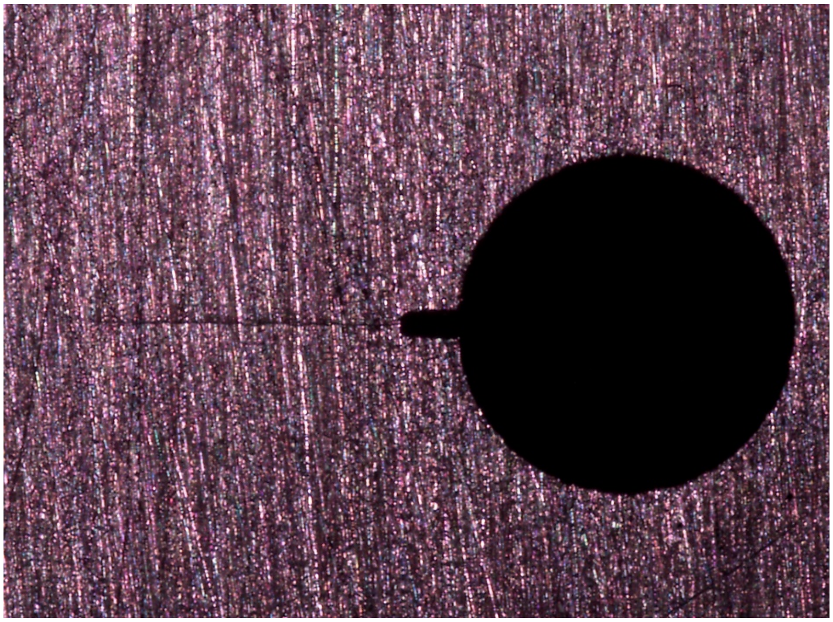

Figure B.5: Crack Shape for λ=-0.5 at 75,000 Cycles in Air Environment.

Figure B.6: Crack Shape for λ=-0.5 at 100,000 Cycles in Saltwater Environment.

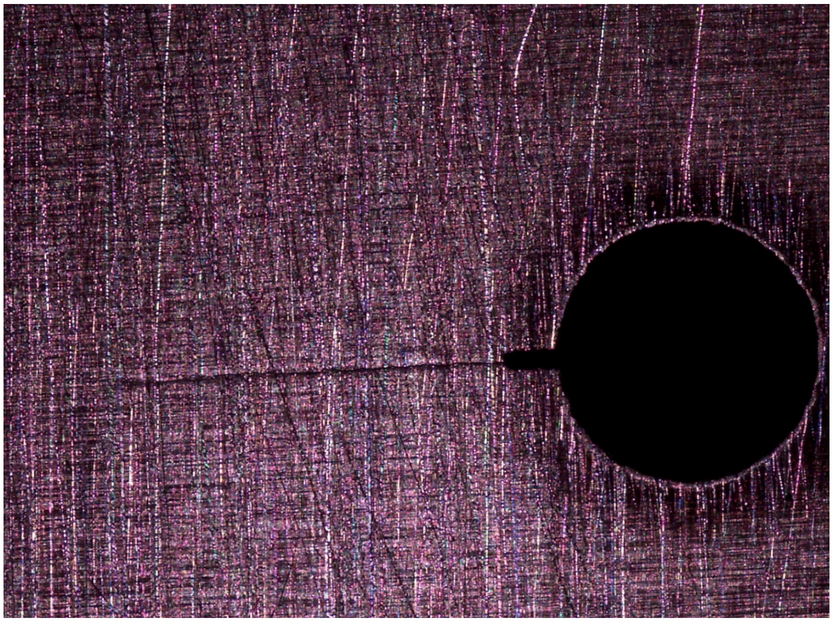

Figure B.7: Crack Shape for λ=-1 at 85,000 Cycles in Air Environment.

Figure B.8: Crack Shape for λ=-1 at 40,000 Cycles in Saltwater Environment.

Appendix C: SEM Images of the Fracture Surfaces

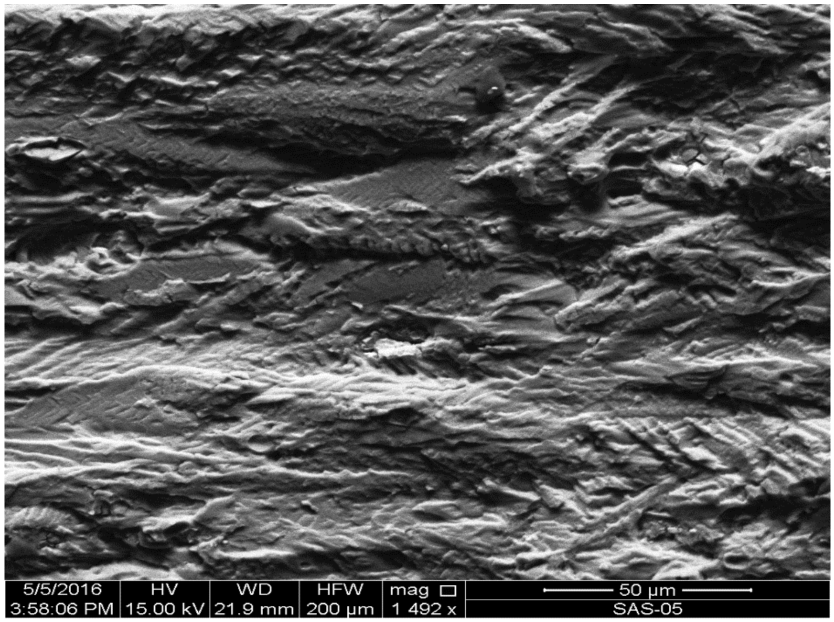

Figure C.1: SEM Image of Fracture Surface for Uniaxial Case in Air Environment.

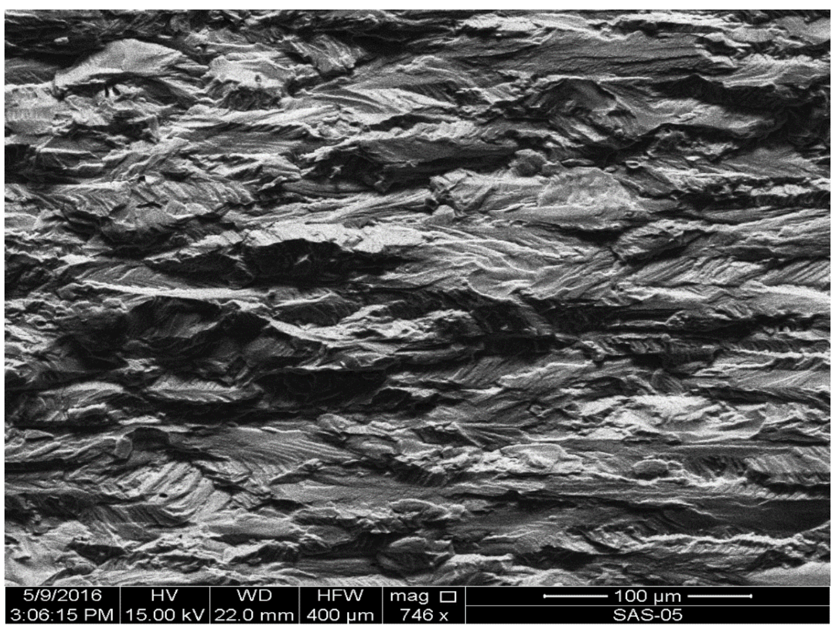

Figure C.2: SEM Image of Fracture Surface for Biaxial Case (λ= 0.5) in Air Environment.

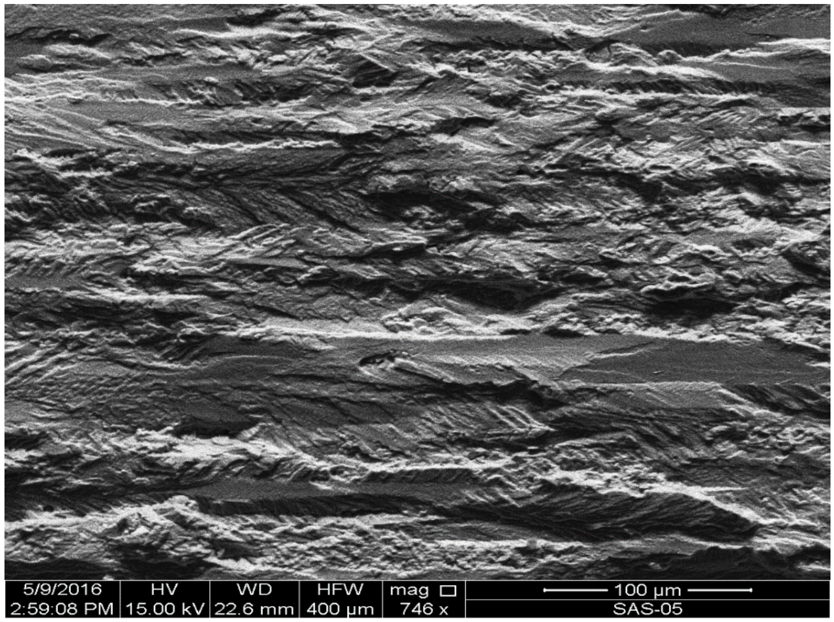

Figure C.3: SEM Image of Fracture Surface for Biaxial Case (λ= -0.5) in Air Environment.

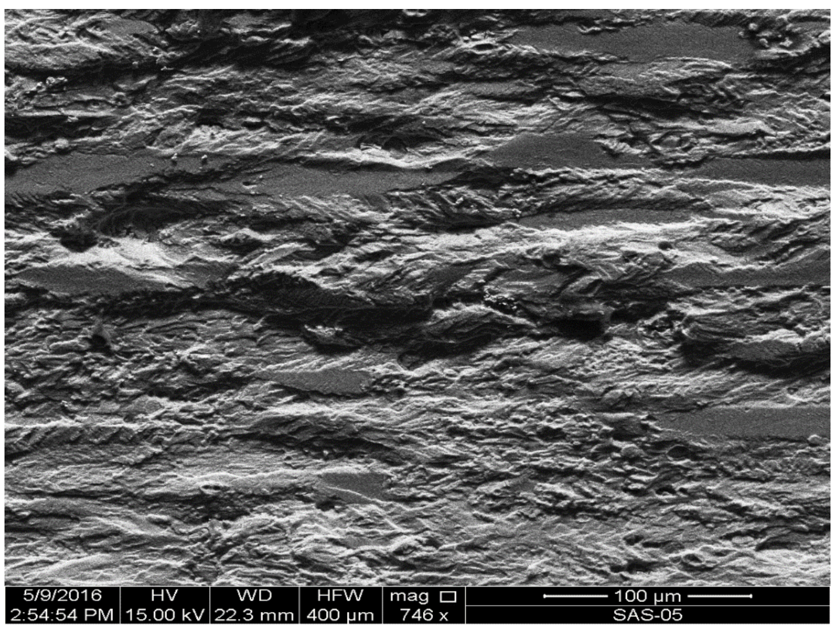

Figure C.4: SEM Image of Fracture Surface for Biaxial Case (λ= -1) in Air Environment.

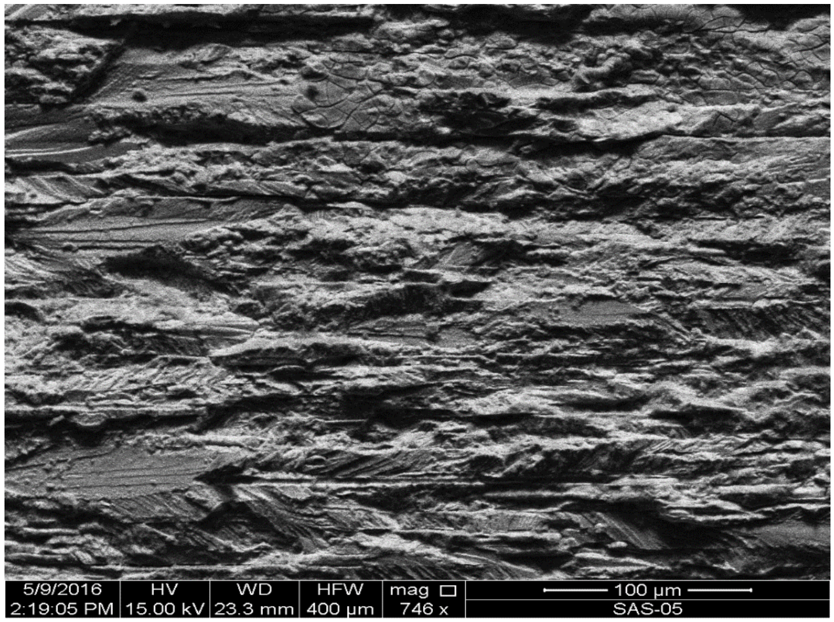

Figure C.5: SEM Image of Fracture Surface for Uniaxial Case in Saltwater Environment.

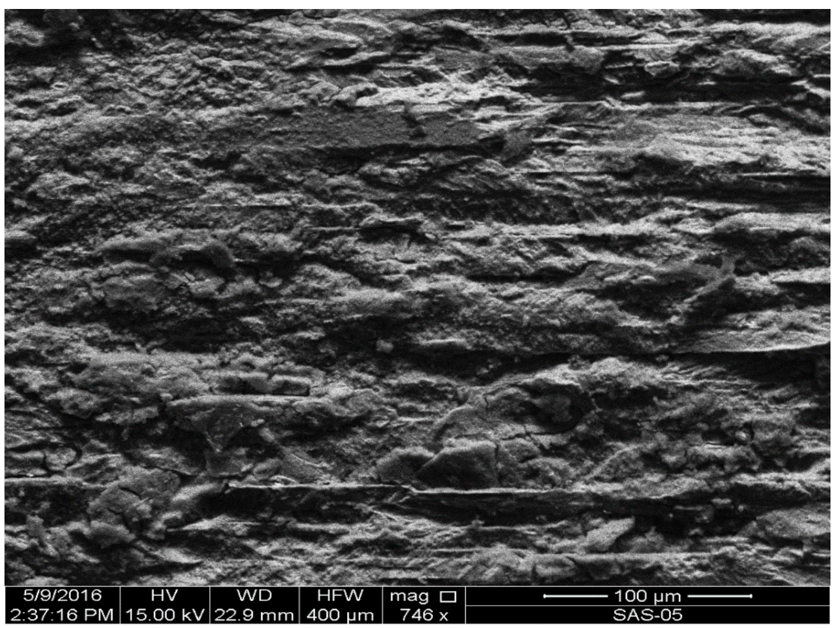

Figure C.6: SEM Image of Fracture Surface for Biaxial Case (λ= 0.5) in Saltwater Environment.

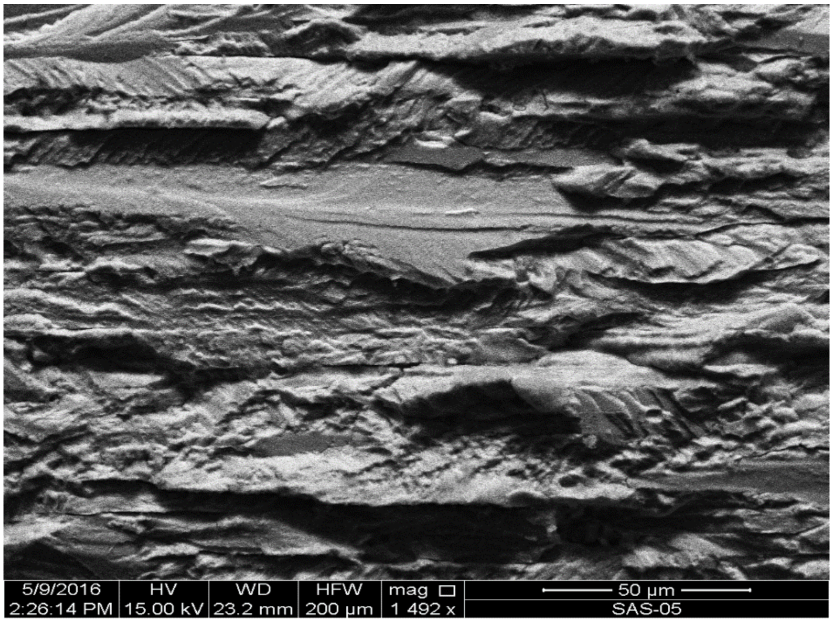

Figure C.7: SEM Image of Fracture Surface for Biaxial Case (λ= -0.5) in Saltwater Environment.

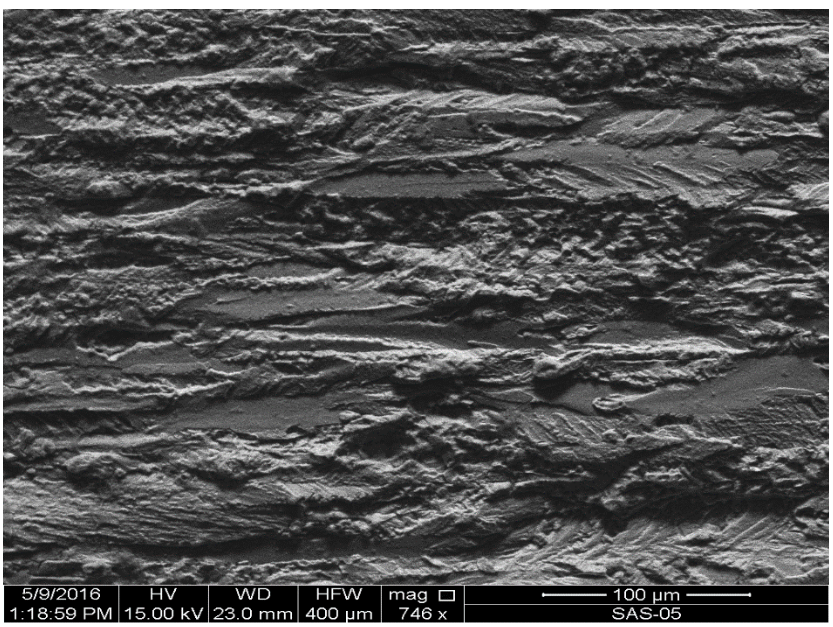

Figure C.8: SEM Image of Fracture Surface for Biaxial Case (λ= -1) in Saltwater Environment.

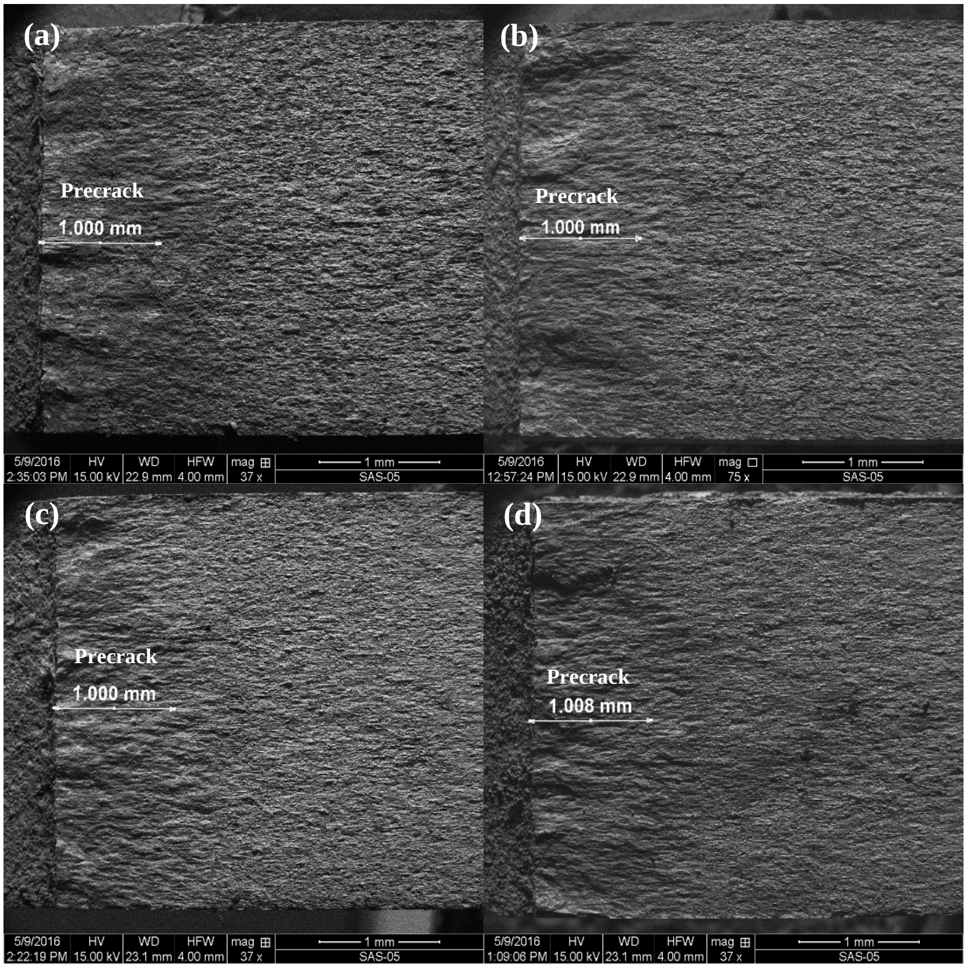

Figure C.9: SEM Images of Fracture Surfaces for Different Biaxial Cases in Saltwater Environment: (a) biaxial (λ= 0.5), (b) uniaxial (λ= 0), (c) biaxial (λ= -0.5), (d) biaxial (λ= -1).

Bibliography

[1] 7000 Series Aluminum Alloy, Aerospace Specification Metals (ASM), http://asm.matweb.com/search/SpecificMaterial.asp?bassnum=MA7075T6. (Accessed November 2014).

[2] AHLUWALIA, HIRA. “Combating Plate Corrosion.” THE FABRICATOR, 2003.

[3] Alcoa 7075 data sheet (PDF). (Accessed August 2nd, 2014).

[4] Anderson, P.R.G., and G.G. Garrett. “Fatigue Crack Growth Rate Variations in Biaxial Stress Fields.” International Journal of Fracture, 16:111–116, 1980.

[5] Anderson, T.L., Fracture Mechanics: Fundamentals and Applications, 3rd edition, Taylor and Francis, 2005.

[6] Berezhnitski, L.T., and R.S. Gromyak. “Evaluation of Limiting State of Matrix in Vicinity of Sharp-Edge Rigid Inclusion.” Material Science, 13-2, 1977.

[7] Davis, JR. “Corrosion of Aluminum and Aluminum Alloys.” Materials Park, OH: ASM International, 1999.

[8] Erdogan, F., and G.C. Sih. “On The Crack Extension in Plates under Plane Loading and Transverse Shear.” Transactions of ASME. Journal of Basic Engineering, 85-4:519-527, 1963.

[9] FHWA. “Corrosion Costs and Preventive Strategies in the United States.” 2002.

[10] Gangloff, P. “Environmental Cracking: Corrosion Fatigue.” Corrosion Tests and Standards Manual ASM International, 1–20, 2004.

[11] Genkin, Jean-Marc P. “Corrosion Fatigue Performance of Alloy 6013-T6.” Massachusetts Institute of Technology, 1992.

[12] Gerhardus, H. Koch. “Aircraft, 2.2 Billion per Year.” 2006.

[13] Hawkins, Kari, Redstone, USAG, “Army Attacks Hardware Corrosion.” The Official Homepage of United States Army, 2012.

[14] Hays, R., and G. Keller. “New Technologies and Future Challenges for the Prevention of Corrosion in US DOD Assets.” U.S. Department Of Defense Corrosion Policy and Oversight Office.

[15] Hopper, C.D., and K.J. Miller. “Fatigue Crack Propagation in Biaxial Stress Fields.” The Journal of Strain Analysis for Engineering Design, 12:23–28, 1977.

[16] Joshi S., J. Shewchuk. “Fatigue-Crack Propagation in a Biaxial-Stress Field.” Exp. Mech., 1970.

[17] Kaminski A.A., and N.S. Sailov. “Spreading Of Cracks from the Contours of Elliptical Openings in Brittle Plates under Biaxial Tensile Stresses.” Soviet Applied Mechanics, 11-2:167-173, 1975.

[18] Kopeliovich, Dmitri. “Corrosion Fatigue.” Knowledge Source on Material Engineering, 2012.

[19] Lados, D.A., and P.C. Paris. “Parameters and Key Trends Affecting Fatigue Crack Growth: a Tribute to Professor Arthur J. Mcevily’s Contributions.” Materials Science and Engineering: A, 468-470:70-73, 2007.

[20] Lee E.U., and R.E. Taylor. “Fatigue Behavior of Aluminum Alloys under Biaxial Loading.” Engineering Fracture Mechanics, 78:1555–1564, 2011.

[21] Liu A.F., and D.F. Dittmer. “Effect of Multiaxial Loading on Crack Growth.” Volume 2: Compilation of Experimental Data, Northrop Corp Hawthorne, 1978.

[22] McEvily, A.J., and W. Illg. “The Rate of Fatigue Crack Propagation in Two Aluminum Alloys.” NASA TN 4394, 1958.

[23] Megson, T.H.G., Aircraft Structures for Engineering Students, 5th edition, P: 371-372, 2012.

[24] Misak H.E., V.Y. Perel, V. Sabelkin, and S. Mall. “Biaxial Tension-Tension Fatigue Crack Growth Behavior of 2024-T3 under Ambient Air and Saltwater Environments.” 2014.

[25] Misak H.E., V.Y. Perel, V. Sabelkin, and S. Mall. “Corrosion Fatigue Crack Growth Behavior of 7075-T6 under Biaxial Tension–Tension Cyclic Loading Condition.” 2013.

[26] Misak H.E., V.Y. Perel, V. Sabelkin, and S. Mall. “Crack Growth Behavior of 7075-T6 under Biaxial Tension–Tension Fatigue.” Int. J Fatigue, 55:158-165, 2013.

[27] Park, J. K., and A.J. Ardell. “Microstructures of the Commercial 7075 Al Alloy in the T651 and T7 Tempers.” Metall. Trans. A, 14:1983, 1957

[28] Parrington, Ronald J. “Fractography of Metals and Plastics.” Practical Failure Analysis, 2002.

[29] Pennisi, Mario S. “Corrosion: Why Apply a Coating.” Coating Fabrication, 1999.

[30] Pocajt, Viktor. “Total Material, Fatigue Properties: Part One.” November 2010.

[31] Ravichandran, K. S., Y. Murakami, and R.O. Ritchie. “Small Fatigue Cracks: Mechanics, Mechanisms and Applications.” ISBN: 0-08-043011-2, 1999.

[32] Rob, Glossary. “Fatigue (Failure Mechanism).” December 2010.

[33] Roberge, P.R. “Corrosion Engineering: Principles and Practice.” McGraw-Hill, 2008.

[34] Roylance, David. “Introduction to Fracture Mechanics.” Department Of Materials Science and Engineering, Massachusetts Institute of Technology, Cambridge, 2001.

[35] Scheel, E. Jeremy, III. Prevéy, S. Paul, and Douglas J. Hornbach. “The Effect of Surface Enhancement on the Corrosion Properties, Fatigue Strength, and Degradation Of Aircraft Aluminum.” Lambda Research, 2010.

[36] Shanyavskiy, A. “Fatigue Cracking Simulation Based on Crack Closure Effects in Al-Based Sheet Materials Subjected to Biaxial Cyclic Loads.” Engineering Fracture Mechanics, 78:1516- 1528, 2011.

[37] Sih, G.C.. “A Special Theory of Crack Propagation.” Mechanics of Fracture, 1:21-45, 1973.

[38] Sih, G.C. and B.C. Cha. “A Fracture Criterion for Three Dimensional Crack Problems.” Engineering Fracture Mechanics, 6:699-723, 1974.

[39] Sunder, R. “Development Of The Marker-TWIST Load Sequence for Quantitative Fractographic Studies.” International Journal of Fatigue, 2010.

[40] Tian, De-Chang, Lu Dau-Quan, and Zhu Jia-Ju. “Crack Propagation under Combined Stresses in Three Dimensional Medium.” Eng.Fract.Mech, 16-1:5-17, 1982.

[41] Tiroshu, J. “Incipient Fracture Angle, Fracture Loci and Critical Stress for Mixed Mode Loading.” Eng.Fract.Mech, 2-3:607-616, 1977.

[42] Uhlig, H.H., and R. Winston Revie. “Corrosion and Corrosion Control.” 4th edition, John Wiley and Sons Inc., 2008.

[43] Wollmann, M. “Structural Integrity: Stress Corrosion Cracking, Corrosion Fatigue.” Universidad Polytecnica de Madrid, Clausthal University of Technology, May 2012.

[44] Yuuki, R., K. Akita, and N. Kishi. “The Effect of Biaxial Stress and Changes of State on Fatigue Crack Growth Behavior.” Fatigue and Fracture of Engineering Materials and Structures, 12:93-103, 1989.

REPORT DOCUMENTATION PAGE	*Form Approved* *OMB No. 0704–0188*

1. REPORT DATE (DD–MM–YYYY)	2. REPORT TYPE	3. DATES COVERED *(From — To)*
18/08/2016	Master's Thesis	August 2014 – September 2016

4. TITLE AND SUBTITLE Corrosion Fatigue Crack Growth Behavior At Notched Hole In 7075-T6 Under Different Biaxial Stress Ratios	5a. CONTRACT NUMBER 5b. GRANT NUMBER 5c. PROGRAM ELEMENT NUMBER
6. AUTHOR(S) Alghamdi, Khalid Ali, Captain, Royal Saudi Air Force	5d. PROJECT NUMBER 5e. TASK NUMBER 5f. WORK UNIT NUMBER
7. PERFORMING ORGANIZATION NAME(S) AND ADDRESS(ES) Air Force Institute of Technology Graduate School of Engineering and Management (AFIT/EN) 2950 Hobson Way WPAFB OH 45433-7765	8. PERFORMING ORGANIZATION REPORT NUMBER AFIT-ENY-MS-16-S-051
9. SPONSORING / MONITORING AGENCY NAME(S) AND ADDRESS(ES) Rich Hays Technical Corrosion Collaboration Office of Secretary of Defense Washington D.C. Tel: (703) 697-3952; E-mail: richard.a.hays18.civ@gmail.com	10. SPONSOR/MONITOR'S ACRONYM(S) TCC OSD 11. SPONSOR/MONITOR'S REPORT NUMBER(S)

12. DISTRIBUTION / AVAILABILITY STATEMENT

Distribution Statement A. Approved For Public Release; Distribution Unlimited.

13. SUPPLEMENTARY NOTES

14. ABSTRACT

This thesis presents the results of a study to quantify the effects of biaxial loading on fatigue crack behavior in both air and saltwater (3.5% NaCl) environments from pre-cracked notched circular hole in a 7075-T6 cruciform specimen using a fracture mechanics approach. With stress ratio of R = 0.5, the crack growth behavior was investigated under fatigue loading with 0.5, 0, -0.5, and -1 biaxial stress ratio λ. The crack propagation was monitored using optical microscopy. Finite Element Analysis was performed using the different stress ranges and stress ratios with various crack sizes to compute of stress intensity factors (ΔK) at the crack tips. It was observed from the study that negative biaxiality has a very pronounced effect on the crack growth rate. The crack propagates faster with negative biaxiality and also the saltwater environment accelerates the crack propagation due to corrosion.

15. SUBJECT TERMS

Corrosion, Fatigue, Fracture Mechanics, Crack Initiation, Crack Growth Rate, Aluminum Alloy

16. SECURITY CLASSIFICATION OF:			17. LIMITATION OF ABSTRACT	18. NUMBER OF PAGES	19a. NAME OF RESPONSIBLE PERSON Shankar, Mall, Ph. D. (ENY)
a. REPORT U	b. ABSTRACT U	c. THIS PAGE U	UU	92	19b. TELEPHONE NUMBER (Include Area Code) (937) 255-6565, ext 4587; Shankar.Mall@afit.edu